

Adult-specific Reelin expression alters striatal neuronal organization. Implications for neuropsychiatric disorders.

1 Mònica Pardo^{1,2}, Sara Gregorio^{1,2,§}, Enrica Montalban³, Lluís Pujadas^{1,2,4,5}, Alba Elias-Tersa^{1,2},
2 Núria Masachs^{1,2}, Alba Vílchez-Acosta^{1,2,#}, Annabelle Parent⁶, Carme Auladell^{1,2}, Jean-
3 Antoine Girault³, Miquel Vila^{2,6,7,8,9}, Angus C Nairn¹⁰, Yasmina Manso^{1,2,†,*} and Eduardo
4 Soriano^{1,2, †,*}

5 ¹ Developmental Neurobiology and Regeneration Lab, Department of Cell Biology, Physiology and
6 Immunology, and Institute of Neurosciences, Universitat de Barcelona, Barcelona 08028, Spain

7 ² Centro de Investigación Biomédica en Red Enfermedades Neurodegenerativas (CIBERNED),
8 Instituto de Salud Carlos III, Madrid 28031, Spain

9 ³ Institut du Fer à Moulin Inserm UMR-S 1270; Inserm, Sorbonne University, 75005 Paris, France

10 ⁴ Department of Experimental Sciences and Methodology, Faculty of Health Science and Welfare,
11 University of Vic - Central University of Catalonia (UVic-UCC), 08500 Vic, Catalonia, Spain

12 ⁵ Tissue Repair and Regeneration Laboratory (TR2Lab); Institute for Research and Innovation in Life
13 and Health Sciences in Central Catalonia (IrisCC), 08500 Vic, Barcelona, Catalonia, Spain.

14 ⁶ Neurodegenerative Diseases Research Group, Vall d'Hebron Research Institute, 08035 Barcelona,
15 Spain

16 ⁷ Department of Biochemistry and Molecular Biology, Autonomous University of Barcelona (UAB),
17 08193 Barcelona, Spain

18 ⁸ Institució Catalana de Recerca i Estudis Avançats (ICREA), 08010 Barcelona, Spain.

19 ⁹ Aligning Science Across Parkinson's (ASAP) Collaborative Research Network, Chevy Chase, MD,
20 USA

21 ¹⁰ Department of Psychiatry, Yale University School of Medicine, New Haven, 06508 Connecticut

22 * **Correspondence:**

23 Eduardo Soriano*

24 esoriano@ub.edu

25 Yasmina Manso*

26 ymansosanz@ub.edu

27 [§] Present address: Institute for Research in Biomedicine (IRB Barcelona), 08025 Barcelona, Spain

28 [#] Present address: Department of Biomedical Sciences, Faculty of Biology and Medicine, University
29 of Lausanne, Lausanne, Vaud, Switzerland.

30 †These authors contributed equally to this work and share last authorship

31 **Keywords: Reelin; Striatum; Interneurons, Dopamine Projections, Schizophrenia, Tourette**
32 **syndrome.**

33 **Abstract**

34 In addition to neuronal migration, brain development and adult plasticity, the extracellular matrix
35 protein Reelin has been extensively implicated in human psychiatric disorders such as schizophrenia,
36 bipolar disorder and autistic spectrum disorder. Moreover, heterozygous *reeler* mice exhibit features
37 reminiscent of these disorders, while overexpression of Reelin protects against its manifestation.
38 However, how Reelin influences the structure and circuits of the striatal complex, a key region for
39 the above-mentioned disorders, is far from being understood, especially when altered Reelin
40 expression levels are found at adult stages. In the present study, we took advantage of
41 complementary conditional gain- and loss-of-function mouse models to investigate how Reelin levels
42 may modify adult brain's striatal structure and neuronal composition. Using immunohistochemical
43 techniques, we determined that Reelin does not seem to influence the striatal patch and matrix
44 organization (studied by μ -opioid receptor immunohistochemistry) nor the density of medium spiny
45 neurons (MSNs, studied with DARPP-32). We show that overexpression of Reelin leads to increased
46 numbers of striatal Parvalbumin- and Cholinergic-interneurons, and to a slight increase in the
47 tyrosine hydroxylase-positive projections. We conclude that increased Reelin levels might modulate
48 the numbers of striatal interneurons and the density of the nigrostriatal dopaminergic projections,
49 suggesting that these changes may be involved in the protection of Reelin against neuropsychiatric
50 disorders.

51 **1 Introduction**

52 Reelin is an extracellular matrix protein important for neuronal migration and layer formation during
53 neocortical development (D'Arcangelo et al., 1995; Alcántara et al., 1998; Rice and Curran, 2001;
54 Soriano and Del Río, 2005; Cooper, 2008; Hirota and Nakajima, 2017; Vílchez-Acosta et al., 2022).
55 Besides its role during development, the Reelin pathway is also active in the adult brain, controlling
56 glutamatergic neurotransmission, dendritic spine formation, synaptic plasticity and adult
57 neurogenesis (Chen et al., 2005; Herz and Chen, 2006; Qiu et al., 2006b; Groc et al., 2007; Niu et al.,
58 2008; Pujadas et al., 2010; Teixeira et al., 2012; Bosch et al., 2016). Reelin binds to Apolipoprotein E
59 Receptor 2 (ApoER2) and Very-Low-Density Lipoprotein Receptor (VLDLR), leading to the
60 phosphorylation and activation of the intracellular adaptor protein Disabled 1 (Dab1), which triggers
61 a complex signalling cascade involving members of the Src kinase family, the PI3K, Erk1/2 and
62 GSK3 kinases, and Cullin-5-dependent degradation, amongst others (Howell et al., 1997, 1999;
63 D'Arcangelo et al., 1999; Hiesberger et al., 1999; Beffert et al., 2002; Arnaud et al., 2003; Benhayon
64 et al., 2003; Ballif et al., 2004; Strasser et al., 2004; González-Billault et al., 2005; Simó et al., 2007,
65 2010; Yasui et al., 2010; Molnár et al., 2019).

66 Genetic studies have associated the Reelin gene (RELN) with a number of psychiatric diseases,
67 including schizophrenia, bipolar disorder and autistic spectrum disorder (Impagnatiello et al., 1998;
68 Fatemi et al., 2001, 2005; Persico et al., 2001; Grayson et al., 2005; Ovidia and Shifman, 2011;
69 Wang et al., 2014; Baek et al., 2015; Lammert and Howell, 2016). This link is also supported by
70 studies showing that Reelin levels are reduced in patients with schizophrenia and bipolar disorder
71 (Fatemi et al., 2000; Torrey et al., 2005; Ruzicka et al., 2007), and can be altered by
72 psychotropic medication (Fatemi et al., 2009). In fact, Reelin haploinsufficiency models, based on

73 the suppression or reduction of Reelin expression (or its downstream pathway), manifest features
74 related to neuropsychiatric disorders, such as cognitive impairments, psychosis vulnerability and
75 learning deficits that frequently coexist with evident alterations in hippocampal plasticity (Tueting et
76 al., 1999; Krueger et al., 2006; Marrone et al., 2006; Qiu et al., 2006a; Ammassari-Teule et al., 2009;
77 Folsom and Fatemi, 2013). Conversely, overexpression of Reelin protects against psychiatric disease-
78 related phenotypes in mice, since it reduces cocaine sensitization, disruption of prepulse inhibition
79 (PPI) and the time spent floating in the forced swim test (Teixeira et al., 2011). Furthermore, Reelin
80 also regulates adult neurogenesis and synaptogenesis (Kim et al., 2002; Pujadas et al., 2010; Teixeira
81 et al., 2012; Bosch et al., 2016), whose disruption is considered to be involved in the pathogenesis of
82 psychiatric disorders (Kempermann, 2008; Zhao et al., 2008).

83 The striatum plays a critical function in motor control and regulation of motivated behaviours (Bolam
84 et al., 2000). Its neuronal population is composed by a 5-10% of interneurons and the rest (90-95%)
85 are GABAergic medium spiny neurons (MSNs). The latter can be classified into striatonigral or
86 striatopallidal subtypes based on their axonal projections to the internal Globus pallidus (iGP) and
87 Substantia Nigra (SN) or to the external Globus Pallidus (eGP), respectively. They can be
88 distinguished by the expression of the Dopamine D1 receptor (striatonigral MSNs) or the Dopamine
89 D2 receptor (striatopallidal MSNs) (Bolam, 1984; Schiffmann et al., 1991; Gerfen, 1992; Smith et
90 al., 1998). Although the striatum exhibits a relatively uniform appearance, it presents a complex
91 organization based in two different compartments: the patches or striosomes (stained by μ -opioid
92 receptor MOR) and the matrix, which surrounds the patches (Olson et al., 1972; Graybiel and
93 Ragsdale, 1978; Herkenham and Pert, 1981). A proper cellular and compartmental organization is
94 essential for a correct striatal function (Crittenden and Graybiel, 2011).

95 Besides the involvement of the striatum (including the Nucleus accumbens) and its circuitry in
96 psychiatric disorders such as major depression, schizophrenia and obsessive-compulsive disorder
97 (OCD), few studies addressing how Reelin influences striatal structure and circuits are available (de
98 Guglielmo et al., 2022). Most of these studies use heterozygous reeler mice as a model, which have
99 reduced Reelin expression also during development. Here we investigate how altering Reelin levels,
100 specifically at late postnatal and adult stages, may lead to cellular and compartmental changes in the
101 striatum that could be related to neuropsychiatric disorders. We used gain- and loss-of-function
102 conditional mouse models to investigate how Reelin levels may modify striatal structure and
103 neuronal composition. Our results suggest that whereas Reelin does not seem to influence the patch-
104 matrix striatal organization and the numbers of MSNs, overexpression of Reelin leads to increased
105 numbers of striatal interneurons and to a slight increase in the dopaminergic projections.

106 **2 Materials and methods**

107 **2.1. Animals**

108 The TgRln is a conditionally regulated transgenic line that overexpresses Reelin by a transactivator
109 (tTA) under the control of the calcium-calmodulin-dependent kinase II α promoter
110 (pCaMKII α) (Pujadas et al., 2010). Reelin transgenic littermates, which have an inactive form of the
111 Reelin gene insertion without the transactivator tTA, were used as controls. For the generation of the
112 Reelin conditional knockout mouse line, homozygous floxed Reelin (fR/fR) mice, with the exon 1 of
113 the Reelin gene flanked by loxP sites, were crossed with a heterozygous UbiCreERT2 line (B6.Cg-
114 Tg(UBC-cre/ESR1)1Ejb/J, stock #008085, The Jackson Laboratory), both on a C57BL/6J
115 background (Vílchez-Acosta et al., 2022). The UbiCreERT2 line displays a ubiquitous expression of
116 the Cre recombinase fused to a modified estrogen receptor ligand-binding domain that retains the Cre

117 at the cytoplasm. Administration of an estrogen receptor antagonist (tamoxifen) induces the nuclear
118 translocation of Cre recombinase and the ubiquitous scission of the floxed gene sequence (ReIn) in
119 all tissues. The resultant offspring (Cre fR/fR) was used for the experiments, and fR/fR littermates
120 were used as controls. In both transgenic lines, 4-5 months old female and male mice were used for
121 the experiments.

122 Male, 8–10-week old, Drd2-EGFP (n=20 Swiss-Webster and 6 C57BL/6N background, founder
123 S118), Drd1a-EGFP (n=4 Swiss-Webster and n=4 C57BL/6N background, founder X60) hemizygous
124 mice were also used in this study. BAC Drd2- and Drd1a-EGFP mice, that express the reporter
125 protein enhanced green fluorescent protein under the control of the D2 and D1 receptor promoters,
126 were generated by GENSAT (Gene Expression Nervous System Atlas) at the Rockefeller University
127 (New York, NY)(Gong et al., 2007).

128 Mice were bred, studied and processed at the animal research facility of the Faculty of Pharmacy of
129 the University of Barcelona and at the animal research facility of the Rockefeller University. Animals
130 were provided with food and water ad libitum and maintained in a temperature-controlled
131 environment in a 12/12 h light-dark cycle. All the experiments involving animals were performed in
132 accordance with the European Community Council directive 2010/63/EU, the National Institute of
133 Health guidelines for the care and use of laboratory animals, and the Rockefeller University's
134 Institutional Animal Care and Use Committee (protocol 14753-H). Experiments were also approved
135 by the local ethical committees.

136 **2.2. PCR Genotyping**

137 DNA was extracted from tail biopsies by adding 100µl Sodium Hydroxide (50mM), and incubating
138 at 100°C during 15 minutes. Then, samples were kept on ice for 10 minutes and stored at -20°C until
139 use.

140 The PCR was performed with the GoTaq® Green Master Mix (Promega), and the primers used for
141 genotyping were as follows. Cre fR/fR line: for homozygous floxed Reelin detection, FloxA
142 (5'CGAGGTGCTCATTTCCTGCACATTGC3') and FloxB (5'
143 CACCGACCAAAGTGCTCCAATCTGTCG 3') primers were used. Homozygous fR/fR mice
144 present only one band of 613 bp whereas heterozygous mice present an additional band at 496 bp. To
145 determine the presence of UbiCre, the primers UbiCre1(5' GCG GTC TGG CAG TAA AAA CTA
146 TC 3') and UbiCre2 (5' GTC AAA CAG CAT TGC TGT CAC TT 3') which are specific for
147 UbiCreERT2, and UbiCre3 (5' CTA GGC CAC AGA ATT GAA AGA TCT 3') and UbiCre4 (5'
148 GTA GGT GGA AAT TCT AGC ATC ATC C 3') as internal positive control were used. Mice
149 heterozygous for Cre (Cre fR/fR) had a double band at 324 and 100 bp while mice negative for Cre
150 only amplified the 100 bp band. TgRln line: the primers RLTG-gen-F (5'-
151 TTGTACCAGGTTCCGCTGGT-3') and RLTG-gen-R (5'-GCA CAT ATC CAG GTT TCA GG-3')
152 were used to amplify both the endogenous Reelin gene (720bp) and the transgenic DNA (320 bp); the
153 primers nTTA-C (5'-ACT AAG TCA TCG CGA TGG AG-3') and nTTA-F (5'-CGA AAT CGT
154 CTA GCG CGT C-3'), were used to detect the transactivator tTA transgene (Pujadas et al., 2010).

155 **2.3. Tamoxifen administration**

156 Inactivation of Reelin expression was induced at postnatal day (p)45-60 by daily intraperitoneal
157 injections of tamoxifen dissolved in 10% alcohol-90% sunflower oil for 3 consecutive days
158 (180mg/kg/day; Sigma-Aldrich).

159 **2.4. Immunohistochemistry**

160 For immunohistochemistry, 4-5 months old mice were perfused transcardially with 4%
161 paraformaldehyde (PFA) in PB 0.1M. Brains were quickly removed, fixed overnight in PFA, and
162 then transferred to 30% sucrose in PBS 0.1M and stored at 4 °C (48h). Brains were frozen with
163 methylbutane (Honeywell) at -42 °C and stored at -80 °C until use. Thirty- μ m coronal sections were
164 obtained with a freezing microtome (Leica SM2010R) and were kept in a cryoprotective solution at -
165 20 °C. Immunohistochemistry was performed on free-floating sections. The sections were inactivated
166 for endogenous peroxidases with 3% H₂O₂ in 10% Methanol and PBS for 15 minutes. After 3 washes
167 with PBS and 3 washes with PBS-0.2% Triton (PBS-T), sections were blocked for 2 h at room
168 temperature (RT) with PBS-T containing 10% of normal horse serum (NHS) and 0.2% of gelatin. For
169 Reelin immunostaining, anti-mouse unconjugated F(ab')₂ fragments (1:300, Jackson
170 ImmunoResearch), were added in the blocking step. After 3 washes with PBS-T, tissue sections were
171 incubated with a primary antibody with PBS-T containing 5% of NHS and 0.2% of gelatine,
172 overnight at 4 °C.

173 The commercial primary antibodies used were: anti-Reelin (clone G10, MAB5364, Merck Millipore,
174 1:1,000), anti-Choline Acetyltransferase (ChAT AB144P, Merck Millipore, 1:500), anti- μ Opioid
175 Receptor (MOR, 1:2000, rabbit, AB5511, Merck Millipore), anti-Parvalbumin (PV, 1:500, Rabbit,
176 PV27, Swant), anti- Dopamine- and cAMP-regulated phosphoprotein, 32 kDa (Darpp32, 1:500,
177 mouse, 611520, BD Transduction Laboratories), anti-Tyrosine Hydroxylase (TH, 1:1000, Rabbit,
178 AB152, Merck Millipore). Sections were washed with PBS-T and then incubated for 2 h at RT with
179 biotinylated secondary antibody (1:200, Vector Laboratories). After subsequent washes with PBS-T,
180 the sections were incubated for 2h at RT with streptavidin-HRP (1:400, GE Healthcare UK). After
181 washing, the staining was developed using 0.03% diaminobenzidine (DAB) and 0.01% H₂O₂, with
182 0.1% nickel ammonium sulphate added to the solution. Finally, sections were dehydrated and
183 mounted with Eukitt mounting medium (Sigma-Aldrich).

184 For immunofluorescence staining a similar procedure was followed using AlexaFluor 488 secondary
185 antibody (1:500, Invitrogen, ThermoFisher) (excluding peroxidase inactivation), counterstained with
186 Bisbenzimidazole (1:500) for 30 minutes at RT, mounted with Mowiol and stored at -20 °C.

187 **2.5. D1-/D2-cell specific mRNA extraction**

188 Cell-type specific translated-mRNA purification (TRAP), was performed as previously described
189 (Heiman et al., 2008) with a few modifications. Each sample consisted of a pool of 2-3 mice. BAC-
190 TRAP transgenic mice (Drd2- and Drd1a-EGFP) were sacrificed by decapitation. The brain was
191 quickly dissected out and placed in a cold buffer and was then transferred to an ice-cold mouse brain
192 matrix to cut thick slices from which the Nucleus Accumbens (NAcc) and the Dorsal Striatum (DS)
193 were punched out using ice-cold stainless-steel cannulas. Each sample was homogenized in 1 ml of
194 lysis buffer (20 mM HEPES KOH [pH 7.4], 5 mM MgCl₂, 150 mM KCl, 0.5mM dithiothreitol, 100
195 μ g/ml CHX protease and RNase inhibitors) with successively loose and tight glass-glass 2 ml
196 Dounce homogenizers. Each homogenate was centrifuged at 2000 x g, at 4 °C, for 10 min. The
197 supernatant was separated from cell debris and supplemented with NP-40 (EDM Biosciences) to a
198 final concentration of 1% and DHPC (Avanti Polar lipids) to a final concentration of 30 mM. After
199 mixing and incubating on ice for 5 minutes, the lysate was centrifuged for 10 minutes at 20,000 x g
200 to separate the supernatant from the insolubilized material. A mixture of streptavidin-coated magnetic
201 beads was incubated with biotinylated protein L and then with GFP antibody that was added to the
202 supernatant and incubated ON at 4 °C with gentle end-over rotation. After incubation, beads were

203 collected with a magnetic rack and washed 5 times with high-salt washing buffer (20 mM HEPES-
204 KOH [pH 7.4], 5 mM MgCl₂, 150 μl 1M, 350 mM KCl, 1% NP-40) and immediately placed in
205 “RTL plus” buffer (Qiagen). The mRNA was purified using the RNase micro KIT (Qiagen). RNA
206 integrity was checked with the Bionalyzer (agilent 2100 Bioanalyzer, Agilent RNA 6000 nano kit).
207 Five ng of mRNA from each sample were used for retro-transcription, performed with the Reverse
208 Transcriptase III (Life Technologies) following the manufacturer’s instructions.

209 **2.6. Real-Time PCR**

210 Quantitative real time PCR, was performed using SYBR Green PCR kit in 96-well plates according
211 to the manufacturer’s instructions. Results are presented as normalized to the indicated house-
212 keeping genes and the delta-threshold cycle (Ct) method was used to obtain a fold change. mRNA
213 levels are presented relative to D2. The housekeeping gene for normalization was beta-myosin heavy
214 chain gene (Myh7).

215 **2.7. Immunohistochemical analysis**

216 For Darpp-32 cell counting, sections were scanned using NanoZoomer 2.0-HT (Hamamatsu). We
217 used FIJI software to crop the striatal profile from the image. Darpp-32 positive cells were counted
218 with the cell nuclei assistant TMarker software.

219 The images of PV and ChAT interneurons were acquired with a Nikon E600 microscope attached to
220 an Olympus DP72 camera, and images were reconstructed using MosaicJ from the Fiji software (Fiji
221 is Just Image J - NIH). The intermediate striatum was subdivided into four sub-regions: Dorso-
222 Medial (DM), Dorso-Lateral (DL), Ventro-Medial (VM) and Ventro-Lateral (VL) (see (Gernert et
223 al., 2000; Ammassari-Teule et al., 2009)) taking slices from Bregma 1.34 mm to 0.02 mm, to identify
224 possible changes in the neuronal distribution inside the different striatal regions. Cell density studies
225 were performed with FIJI tools to measure the area and to count cells (cell counter).

226 To measure TH intensity, slides were scanned with SilverFast at 600ppm and SigmaPlot was used to
227 measure the intensity of the different striatal areas. The results are expressed as % from control which
228 was considered as 1 in each independent experiment to avoid deviations caused by differences in the
229 DAB development procedure.

230 Synaptic bouton images were taken with 63X oil immersion objective and counted selecting
231 randomly an 11x11 mm² ROI using Fiji.

232 For each mouse transgenic line we analyzed 3-14 animals and for each animal and average of 6-8
233 images were analyzed.

234 **2.8. Statistics**

235 All statistical analyses were performed using Graphpad Prism 5.0 software (GraphPad Software,
236 Inc). Data was analyzed with unpaired two-tailed Student’s T-tests and statistical significance was set
237 at p-value <0.05. Unless otherwise stated, all values are presented as mean ± the standard error of the
238 mean (SEM). The number of animals used in each experiment is detailed in the figure legend.

239

240 **3 Results**

241 **3.1. Reelin is highly expressed in striatonigral MSNs**

242 To determine the effects of Reelin levels in the mouse striatal organization, we first studied Reelin
243 expression in a Reelin overexpressing and a knock out mouse line. Control mice from both lines
244 exhibited numerous Reelin-positive cell bodies that were distributed throughout the striatum (Figure
245 1A, C), whereas the tamoxifen-inducible conditional knockout mouse line (Cre fR/fR) presented a
246 drastic reduction of Reelin protein as detected by immunohistochemistry (Figure 1B) and by western
247 blot (not shown). In contrast, Reelin overexpressing mice (TgRln) showed a dramatic increase of
248 Reelin protein in the striatum (Figure 1D) which was apparent in both the cell bodies and in the
249 neuropil (see also (Pujadas et al., 2010)).

250 Reelin has been described to co-localize with Calbindin D-28k-positive neurons (Sharaf et al., 2015),
251 a well-known marker of striatal MSNs. Hence, we used the TRAP technology (Heiman et al., 2008)
252 to determine a possible enrichment of Reelin mRNA in D1- or D2- receptor expressing MSNs in both
253 DS and NAcc. BAC-TRAP-D1 and -D2 mice, were used to specifically immunoprecipitate mRNAs
254 from D1 (striatonigral) or D2 (striatopallidal) neuronal populations from the DS and the NAcc.
255 Reelin mRNA levels were compared to the housekeeping beta-myosin heavy chain gene. Results
256 indicated that Reelin mRNA is enriched in D1-MSNs, in both the DS and the NAcc (Figure 1E, F).
257 The expression of Dab1, a key downstream effector of the Reelin pathway, was also higher in D1
258 MSNs of the DS and NAcc (Figure 1G, H). These results suggest that the striatonigral D1 MSNs
259 population is the main producer of striatal Reelin.

260 **3.2. Striatal MSNs organization is independent of Reelin expression levels.**

261 To determine whether Reelin expression levels could modify DS MSN populations, we first
262 immunostained sections with Darpp-32, a marker of MSNs, and quantified the density of striatal
263 MSNs in the Cre fR/fR (Figure 2A, B) and TgRln (Figure 2C, D) mouse models. Results indicated
264 that neither the absence nor the overexpression of Reelin altered the density of striatal Darpp-32
265 positive neurons in the striatum of Cre fR/fR (Figure 2A-B, E) or TgRln mice (Figure 2C-D,F).

266 Since Reelin controls neuronal migration, we next wanted to determine whether Reelin levels could
267 affect the DS patch organization. Immunostaining of the striosomes with MOR showed striatal
268 patches with a similar spatial distribution in all genotypes, suggesting that striatal MSNs density and
269 organization are not affected by alterations of Reelin expression levels (Figure 2G-I).

270 **3.3. Reelin overexpression alters striatal interneuron population**

271 In addition to MSNs, the striatum also contains ChAT-positive and GABAergic interneurons, being
272 the PV-expressing ones the best known. To assess the number and distribution of ChAT-positive
273 interneurons in the different transgenic lines, we subdivided the DS in four Dorso-Ventral and
274 Medio-Lateral regions (Figure 3A). Analysis of the density and distribution of ChAT-positive cells
275 showed no differences in Cre fR/fR mice compared to controls (Figure 3A-F). In contrast, the density
276 of ChAT-positive cells was increased in Reelin overexpressing mice compared to controls, reaching
277 significance in 3 of the striatal sub-regions analyzed (Figure 3G-L)

278 We also analyzed the density and distribution of PV striatal interneurons. In line with the ChAT-
279 positive interneuron data, no changes in the density and distribution of PV-positive interneurons
280 (Figure 4A-B) were observed in any of the DS regions of Cre fR/fR mice compared to controls

281 (Figure 4C-F). However, analysis of PV-positive interneurons density in TgRln mice showed a
282 statistically significant increase in the VL striatum (Figure 4G, H, K) but not in other striatal regions
283 (Figure 4 G-J, L) as compared to controls. Altogether, our results indicated that Reelin
284 overexpression increased the number of DS interneurons.

285 **3.4. Reelin levels control dopaminergic projections**

286 Next, we analyzed whether the expression of Reelin could influence dopaminergic projections. Thus,
287 we performed immunohistochemistry for TH to detect dopaminergic projections that reach the
288 striatum from the Substantia Nigra (SN) and the Ventral Tegmental Area (VTA). We quantified TH
289 intensity in the DS and the Ventral Striatum (VS), including the NAcc and the Olfactory Tubercle
290 (OT). In the Cre fR/fR model, we observed no alterations in the dopaminergic intensity in none of the
291 three striatal regions studied (Figure 5A-E) compared to controls. However, in the OT of Cre fR/fR
292 mice, we observed a tendency towards a reduction in TH intensity compared to controls (Figure 5E).
293 In contrast, in Reelin overexpressing mice, quantification of TH immunostaining (Figure 5F-G)
294 showed a significant increase of TH intensity in both the NAcc and OT regions compared to controls
295 (Figure 5H-J).

296 Finally, we also wanted to quantify synaptic boutons of striatal dopaminergic projections. Thus, we
297 determined the density of synaptic boutons in the DS, NAcc and OT, dividing the DS into Dorsal and
298 Ventral regions. In the Cre fR/fR mice, the density of synaptic boutons in all the regions was similar
299 to that of control mice (DS dorsal: fR/fR 0.2838 ± 0.017 vs. Cre fR/fR 0.3025 ± 0.014 ; DS ventral:
300 fR/fR 0.2720 ± 0.016 vs. Cre fR/fR 0.2688 ± 0.023 ; NAcc: fR/fR 0.2618 ± 0.013 vs. Cre fR/fR
301 0.2530 ± 0.034 ; OT: fR/fR 0.2428 ± 0.013 vs. Cre fR/fR 0.2493 ± 0.018 ; $n = 4$ mice/genotype,
302 Mean \pm SD). In contrast, the density of dopaminergic synaptic boutons tended to increase in the TgRln
303 mice compared to controls (Figure 6A-L), being statistically significant in the NAcc (Fig. 6C, G, K).
304 These results suggest that higher Reelin levels might modulate dopaminergic fibres and synaptic
305 boutons, mainly in the NAcc.

306

307 **4 Discussion**

308 Variations in Reelin expression levels have been shown to be important for the development of
309 neuropsychiatric disorders (Impagnatiello et al., 1998; Fatemi et al., 2000, 2001, 2005; Persico et al.,
310 2001; Torrey et al., 2005; Grayson et al., 2005; Ruzicka et al., 2007; Ovadia and Shifman, 2011;
311 Wang et al., 2014; Baek et al., 2015; Lammert and Howell, 2016); however, we still lack the precise
312 understanding of the mechanistic insights of this correlation. Here we focused our attention on the
313 striatum as a key region participating in the pathogenesis of psychiatric diseases (McCutcheon et al.,
314 2021). We thus characterized specific striatal neuronal populations as well as the dopaminergic
315 mesolimbic innervation in two different mouse models either overexpressing or deficient for Reelin.
316 In previous studies we reported that TgRln mice were more resilient to stressors implicated in the
317 genesis of psychiatric diseases (chronic stress and psychostimulant administration) (Teixeira et al.,
318 2011), suggesting a role for Reelin in preventing behavioral symptoms related with these disorders.
319 Here we show that Reelin-depletion at adult stages does not lead to significant changes neither in the
320 striatal composition nor in the dopaminergic innervation, while postnatal Reelin overexpression
321 increases interneuron populations as well as the density of dopaminergic striatal projections from the
322 VTA. Together, our results suggest the participation of postnatal Reelin expression in the fine
323 structural tuning of the striatal area (Figure 7).

324 **4. 1 A role for Reelin in the striatum.**

325 The role of Reelin in the cortex and the hippocampus has been extensively studied including the
326 expression pattern in GABAergic interneurons and the regulation in glutamatergic synapses
327 (Alcántara et al., 1998; Herz and Chen, 2006; Jossin, 2020). Indeed, it has been characterized that
328 Reelin controls several structural and functional properties of the glutamatergic synapses including
329 the strength of glutamate neurotransmission (Beffert et al., 2005; Qiu et al., 2006b), protein
330 composition at presynaptic boutons (Hellwig et al., 2011), structural properties of dendritic spines
331 (Bosch et al., 2016) as well as trafficking of glutamate receptor subunits (Sinagra et al., 2005; Groc et
332 al., 2007). Several studies also support a key role of Reelin in the correct organization of the basal
333 ganglia. For instance, blockade of Reelin or its signaling pathway leads to a severe disorganization of
334 the tangentially migrating midbrain dopaminergic (mDA) neurons, which fail to reach their final
335 position in the SN pars compacta (SNc) and accumulate instead in the VTA. This results in a
336 conspicuous reduction of the number of mDA neurons in the SNc, despite no overall changes in the
337 number of mDA neurons have been described (Nishikawa et al., 2003; Kang et al., 2010; Sharaf et
338 al., 2013; Bodea et al., 2014). Interestingly, alterations in the radial and tangential fibers that guide
339 migrating mDA neurons have been described in *reeler* mice (Nishikawa et al., 2003; Kang et al.,
340 2010) and support the idea that Reelin might also be guiding mDA neuronal migration indirectly by
341 controlling the normal development of guidance scaffolds. However, specific inactivation of Reelin
342 signaling in mDA neurons indicates a direct role of Reelin in the tangential migration of this neuronal
343 population towards the SNc by promoting fast-laterally-directed migration and stabilization of their
344 leading process (Vaswani et al., 2019). Despite these organization abnormalities in the SNc, no
345 significant alterations have been described in the nigrostriatal pathway of *reeler*, *reeler-like* mutants
346 or heterozygous *reeler* mice (Nishikawa et al., 2003; Sharaf et al., 2013; Vaswani et al., 2019). In
347 contrast, defects in cortico-striatal plasticity (Marrone et al., 2006) and in the dopaminergic system
348 (Matsuzaki et al., 2007) have been reported in *reeler* mice. Moreover, alterations in striatal
349 composition, such as reductions in the number of striatal PV+ neurons along the rostro-caudal axis
350 (Marrone et al., 2006; Ammassari-Teule et al., 2009), decreases in TH immunoreactivity in the NAcc
351 (Nullmeier et al., 2014) and increases in the density of ChAT (Sigala et al., 2007) and the expression
352 of D1, D2 and serotonin 5-HT_{2A} receptors (Matsuzaki et al., 2007; Varela et al., 2015) when Reelin
353 levels are decreased, have been also described.

354 In this study we describe a preferential expression of Reelin mRNA in a specific subpopulation of
355 MSNs of the striatum, the D1 neurons, corroborating previous studies using FISH (de Guglielmo et
356 al., 2022). Further, the fact that both Reelin and *Dab1* expression are higher in striatonigral D1 MSNs
357 than in striatopallidal D2 MSNs, suggests that Reelin may function in an autocrine manner in D1
358 MSNs.

359 Nevertheless, the lack of Reelin during development does not lead to dramatic alterations in the
360 striatum of *reeler* mice. Considering the low Reelin expression levels in the midbrain and the
361 profound defects associated with its absence, it has been hypothesized that Reelin may not act only
362 by simple diffusion but also by axonal transport to target other brain structures (Nishikawa et al.,
363 2003). The possibility that Reelin may be transported from a region such as the striatum to the SN or
364 VTA is thus feasible and may represent the primary source of Reelin for midbrain neurons. Indeed,
365 the idea that Reelin is anterogradely transported through striatonigral fibers of D1 MSNs to act on
366 dopaminergic neurons seems to be relevant during migration but uncertain in adulthood since Reelin
367 canonical receptors (i.e. ApoER2 and VLDLR) are not expressed in the adult midbrain (Sharaf et al.,
368 2015). Considering the previous data, the specific effect of postnatal alterations of Reelin levels has
369 been studied in detail in the striatum and interconnected areas including the SN and the VTA.

370 **4. 2 Consequences of the deficit of Reelin in psychiatric disorders.**

371 The description of heterozygous *reeler* mice as a useful model of psychosis vulnerability is still
372 controversial since the phenotypic behavioral alterations observed could be attributable either to a
373 role of Reelin during development or to an acute effect at adult stages. Given that very few studies
374 have addressed this issue (Matsuzaki et al., 2007), here we use a conditional KO model (Cre fR/fR)
375 in which neurodevelopment is preserved, which allowed us to specifically analyze the contribution of
376 adult Reelin expression to the cellular and anatomical organization of the striatum. Previous studies
377 have shown that in *reeler* and heterozygous-*reeler* mice there was a decrease in the density of PV+
378 cells in the Dorsal-Medial and Ventral-Medial striatal regions (Marrone et al., 2006; Ammassari-
379 Teule et al., 2009). However, in Cre fR/fR mice we found no significant changes in cell densities of
380 CHAT+ and PV+ interneurons. These differences can be attributable to the fact that in previous
381 studies the lack of Reelin started during development, whereas in our study Reelin inactivation takes
382 place at adult stages. In sum, these data suggest that Reelin expression is critical for striatal PV+
383 interneuron formation during striatal development, but not for maintenance of the pool of such
384 interneuron populations during adulthood.

385 Similarly, previous studies evidenced alterations in TH expression in VTA and reduction in TH+
386 immunoreactivity terminals in striatum and VTA in heterozygous Reeler mice (Ballmaier et al.,
387 2002). To analyze the effect of adult Reelin depletion, we mapped TH+ immunoreactivity in
388 striatum, VTA and NAcc areas in Cre fR/fR mice, finding no differences with controls, although
389 there was a trend in the OT. Our data suggests that at adult stages Reelin is largely dispensable for
390 the maintenance of the dopaminergic innervation from the SN/VTA to the striatum.

391

392 **4. 3 Reelin overexpression in the striatum and drug sensitization.**

393 Although it has been widely described that the mesolimbic system controls drug sensitization, there
394 are studies involving other striatal elements, such as the striatal patch-matrix organization and striatal
395 interneurons, in the control of this process. We already reported that Reelin overexpression leads to
396 reduced sensitization to cocaine (Teixeira et al., 2011). The characterization of the striatal
397 organization in TgRln mice is essential to further understand the mechanisms underlying drug
398 sensitization. Despite the fact that the gross structure of the striatal architecture was not altered in
399 TgRln mice, the study of striatal interneurons, which represent 5% of the striatal cell population,
400 clearly suggests that Reelin is able to modulate interneuron densities. For instance, Reelin
401 overexpression leads to increased densities of PV+ and ChAT+ cells, suggesting a specific response
402 of these neurons to increased amounts of Reelin. In addition, our results clearly indicate an increase
403 of dopaminergic fibers in the NAcc and Olfactory tubercle of the TgRln mice. These alterations
404 found in TgRln mice, but not in Cre fR/fR mice, reinforce the notion that increased Reelin levels
405 modulate the striatal cytoarchitecture while Reelin presence in adulthood is not essential for the
406 maintenance of the striatal organization.

407 Interestingly, decreased density of PV+ interneurons in the dorsomedial and ventromedial striatum of
408 heterozygous *reeler* mice have been paralleled with deficits in some behaviors strongly disrupted in
409 schizophrenic patients (Ammassari-Teule et al., 2009). Moreover, cocaine sensitization correlates
410 with transient increases in the number of PV+ neurons in striatum that become reduced beyond
411 normality after a 2-week cocaine withdrawal period (Todtenkopf et al., 2004). The fact that TgRln
412 mice, which show reduced sensitization to cocaine, also show increased densities of PV+

413 interneurons could be apparently contradictory; nevertheless, here the number of PV+ interneurons is
414 sustained, while upon cocaine administration the increase is transient, and eventually, related to
415 compensatory responses. Anyhow, the fact that changes in PV+ interneuron number are controlling
416 cocaine sensitization suggests that the increased density of PV+ cells observed in TgRln mice could
417 be involved in the reduction of cocaine sensitization described in these mice (Teixeira et al., 2011).
418 Although the mechanisms by which Reelin overexpression leads to increased numbers of PV and
419 CHAT neurons remain unknown, it is important to remark that CAMKII promoter drives expression
420 of Reelin in the striatum from the end of the first postnatal week onwards. It is thus possible that
421 Reelin influences positively the maturation and survival of these interneurons, through Reelin/Dab1
422 associated pathways that influence these processes (Simó et al., 2007; Lee et al., 2014).

423 **4.4 Molecular mechanisms of the effect of Reelin in the mesolimbic system.**

424 Disturbances in the dopaminergic mesolimbic system including altered immunoreactivity and mRNA
425 levels of TH and dopamine transporters (D2, D3) in the VTA and the ventral striatum have been
426 reported in heterozygous *reeler* mice (Ballmaier et al., 2002) and could be related to some of the
427 behavioral deficits observed in this model. It has been described that after cocaine administration,
428 there is an specific increase in the ERK pathway in striatonigral MSNs (Bertran-Gonzalez et al.,
429 2008), a pathway that is also activated by Reelin (Simó et al., 2007; Lee et al., 2014). Interestingly,
430 an increased Fos activation in the dorsal medial striatum but not in the NAcc of heterozygous *reeler*
431 mice after the administration of cocaine has been described (de Guglielmo et al., 2022). Increases in
432 Fos activation are thought to be the result of the cocaine-induced upregulation in dopamine levels in
433 the striatum (Di Chiara and Imperato, 1988) which is hypothesized that might increase the activity of
434 MSNs by activating D1 and D2 receptors. Experiments in mice lacking D1 receptor evidence a clear
435 role for this receptor in the psychomotor effects of cocaine. As mentioned before, our data and that of
436 others (de Guglielmo et al., 2022) evidences a preferential expression of Reelin in D1 neurons,
437 supporting the idea that Reelin could be somehow modulating its function and hence influencing
438 cocaine-induced psychomotor effects which are reduced in Reelin overexpressing mice (Teixeira et
439 al., 2011) and increased when Reelin levels are reduced (de Guglielmo et al., 2022).

440 Specific Reelin activation in striatal neurons has not been proved so far, and additionally it has been
441 described that expression of Reelin canonical receptors ApoER2 and to a lesser extent VLDLR is
442 reduced in mature midbrain and striatum. From this data it can be assumed that Reelin functions are
443 mostly restricted to migratory events and early postnatal maturation and that it is dispensable for the
444 maintenance of dopaminergic neurons. Nevertheless, the putative contribution of the non-canonical
445 Reelin pathway in ERK activation (Lee et al., 2014) maintains the potentiality of Reelin as a relevant
446 factor. Together, we propose that Reelin overexpression in striatonigral MSNs could be controlling
447 the ERK pathway and its feedback modulation to down regulate some responses to drug abuse.

448 Also interesting is the fact that the mesolimbic system is critical to induce drug sensitization (for
449 example amphetamine (Perugini and Vezina, 1994)) which leads to a higher expression of c-fos
450 positive cells in striatal patches rather than in the matrix compartment (Graybiel et al., 1990). Since
451 Reelin has been described to be selectively expressed in striatal patches (Alcántara et al., 1998;
452 Nishikawa et al., 1999) and Reelin controls immediate-early gene expression including *Egr-1*, *Arc*
453 and *c-fos* amongst others (Simó et al., 2007; Stritt and Knöll, 2010) we could not discard that higher
454 expression of Reelin in TgRln mice triggers reduced drug sensitization through the mediation of *c-fos*
455 levels in striatal patches. Exploration of this eventuality will require specific research.

456 **4.5 Reelin as a possible therapeutic target for psychiatric diseases.**

457 Reelin has been placed as a top candidate gene associated with several neuropsychiatric diseases.
458 This link is supported by several studies showing that Reelin levels are reduced in patients with
459 schizophrenia, bipolar disorder and autistic spectrum disorder (Impagnatiello et al., 1998; Fatemi et
460 al., 2000, 2001, 2005; Persico et al., 2001; Torrey et al., 2005; Grayson et al., 2005; Ruzicka et al.,
461 2007; Ovadia and Shifman, 2011; Wang et al., 2014; Baek et al., 2015; Lammert and Howell, 2016).
462 Schizophrenia, which presents behavioral sensitization, can be compared with phenotypes related to
463 drug sensitization where the protective effect of Reelin overexpression has been demonstrated
464 (Teixeira et al., 2011). Moreover, in schizophrenic patients it has been described that densities of
465 ChAT+ cell profiles were significantly reduced in the caudate nucleus, the ventral striatum and in the
466 striatum as a whole in the schizophrenic group (Holt et al., 1999). Thus, Reelin overexpression may
467 potentially counteract cholinergic interneuron alterations in schizophrenic patients.

468 It is interesting to notice that the striatal changes observed in TgRln mice are opposite to those found
469 in patients with Tourette's syndrome which present a clear decrease in the density of PV+ and
470 ChAT+ interneurons in the dorsal striatum with no alterations in the density and number of MSNs
471 (Kataoka et al., 2010). In TgRln mice, increased densities of PV+ and ChAT+ striatal interneurons
472 with no overall alterations in the density of MSNs have been described. Importantly, the etiology of
473 Tourette's syndrome is heterogeneous and complex, with unclear mechanistic contributions, but with
474 apparent dysfunction of interneurons functioning (Rapanelli et al., 2017), making it hard to find an
475 effective treatment. Noteworthy, GWAS studies have identified RELN genetic variants in Tourette's
476 syndrome (Li et al., 2012) and together with our findings in the TgRln model suggest that Reelin
477 could be an attractive therapeutic approach to reverse the symptoms of this disorder, although altered
478 Reelin expression or signaling should be explored in patients affected by Tourette's syndrome. The
479 finding that adult-depletion of Reelin does not provoke significant alterations in striatum, but that
480 Reelin overexpression induces changes in interneuron populations and dopaminergic innervations,
481 positions Reelin fragments or pharmacological tools as top candidates for being used in future
482 therapies.

483 **5 Conflict of Interest**

484 The authors declare that the research was conducted in the absence of any commercial or financial
485 relationships that could be construed as a potential conflict of interest.

486 **6 Author Contributions**

487 ES contributed to conception and design of the study. MP, SG, EM, LP, AE, NM, AV and YM
488 performed the experiments. MP, SG, EM, CA and YM analyzed the data and performed statistical
489 analysis. AN contributed new reagents/analytic tools, MP, LP, YM and ES wrote the first draft of the
490 manuscript. EM, AP, JG, CA and MV wrote sections of the manuscript. YM and ES reviewed and
491 edited the final version. All authors contributed to manuscript revision, read, and approved the
492 submitted version.

493 **7 Funding**

494 This work was supported by grants from the Spanish MINECO and MICIN (SAF2016-76340R and
495 PID2019-106764RB-C21, Excellence Unit 629, María de Maeztu/Institute of Neurosciences), and by
496 CIBERNED (ISCIII, Spanish Ministry of Health) to E.S; Aligning Science Across Parkinson's
497 through The Michael J. Fox Foundation for Parkinson's Research, USA (ASAP-020505 to M.V.),
498 Ministry of Science and Innovation (MICINN), Spain (PID2020-116339RB-I00 to M.V.), EU Joint

499 Programme Neurodegenerative Disease Research (JPND), Instituto de Salud Carlos III, EU/Spain
500 (AC20/00121 to M.V.).

501

502 **8 Acknowledgments**

503 We thank Daniela Rossi and Ashraf Muhaisen for help in the management of mouse colonies.

504 **References**

505 Alcántara, S., Ruiz, M., D’Arcangelo, G., Ezan, F., de Lecea, L., Curran, T., et al. (1998). Regional
506 and cellular patterns of reelin mRNA expression in the forebrain of the developing and adult
507 mouse. *J. Neurosci.* 18, 7779–7799. doi: 10.1523/JNEUROSCI.18-19-07779.1998.

508 Ammassari-Teule, M., Sgobio, C., Biamonte, F., Marrone, C., Mercuri, N. B., and Keller, F. (2009).
509 Reelin haploinsufficiency reduces the density of PV+ neurons in circumscribed regions of the
510 striatum and selectively alters striatal-based behaviors. *Psychopharmacology (Berl)*. 204, 511–
511 521. doi: 10.1007/s00213-009-1483-x.

512 Arnaud, L., Ballif, B. A., and Cooper, J. A. (2003). Regulation of protein tyrosine kinase signaling by
513 substrate degradation during brain development. *Mol. Cell. Biol.* 23, 9293–9302. doi:
514 10.1128/MCB.23.24.9293-9302.2003.

515 Baek, S. T., Copeland, B., Yun, E.-J., Kwon, S.-K., Guemez-Gamboa, A., Schaffer, A. E., et al.
516 (2015). An AKT3-FOXG1-reelin network underlies defective migration in human focal
517 malformations of cortical development. *Nat. Med.* 21, 1445–1454. doi: 10.1038/nm.3982.

518 Ballif, B. A., Arnaud, L., Arthur, W. T., Guris, D., Imamoto, A., and Cooper, J. A. (2004). Activation
519 of a Dab1/CrkL/C3G/Rap1 pathway in Reelin-stimulated neurons. *Curr. Biol.* 14, 606–610. doi:
520 10.1016/j.cub.2004.03.038.

521 Ballmaier, M., Zoli, M., Leo, G., Agnati, L. F., and Spano, P. (2002). Preferential alterations in the
522 mesolimbic dopamine pathway of heterozygous reeler mice: an emerging animal-based model
523 of schizophrenia. *Eur. J. Neurosci.* 15, 1197–1205. doi: 10.1046/j.1460-9568.2002.01952.x.

524 Beffert, U., Morfini, G., Bock, H. H., Reyna, H., Brady, S. T., and Herz, J. (2002). Reelin-mediated
525 signaling locally regulates protein kinase B/Akt and glycogen synthase kinase 3beta. *J. Biol.*
526 *Chem.* 277, 49958–49964. doi: 10.1074/jbc.M209205200.

527 Beffert, U., Weeber, E. J., Durudas, A., Qiu, S., Masiulis, I., Sweatt, J. D., et al. (2005). Modulation
528 of Synaptic Plasticity and Memory by Reelin Involves Differential Splicing of the Lipoprotein
529 Receptor Apoer2. *Neuron* 47, 567–579. doi: 10.1016/j.neuron.2005.07.007.

530 Benhayon, D., Magdaleno, S., and Curran, T. (2003). Binding of purified Reelin to ApoER2 and
531 VLDLR mediates tyrosine phosphorylation of Disabled-1. *Brain Res. Mol. Brain Res.* 112, 33–
532 45.

533 Bertran-Gonzalez, J., Bosch, C., Maroteaux, M., Matamales, M., Hervé, D., Valjent, E., et al. (2008).
534 Opposing Patterns of Signaling Activation in Dopamine D1 and D2 Receptor-Expressing

- 535 Striatal Neurons in Response to Cocaine and Haloperidol. *J. Neurosci.* 28.
- 536 Bodea, G. O., Spille, J.-H., Abe, P., Andersson, A. S., Acker-Palmer, A., Stumm, R., et al. (2014).
537 Reelin and CXCL12 regulate distinct migratory behaviors during the development of the
538 dopaminergic system. *Development* 141, 661–673. doi: 10.1242/dev.099937.
- 539 Bolam, J. P. (1984). Synapses of identified neurons in the neostriatum. *Ciba Found. Symp.* 107, 30–
540 47.
- 541 Bolam, J. P., Hanley, J. J., Booth, P. A., and Bevan, M. D. (2000). Synaptic organisation of the basal
542 ganglia. *J. Anat.*, 527–42.
- 543 Bosch, C., Masachs, N., Exposito-Alonso, D., Martínez, A., Teixeira, C. M., Fernaud, I., et al.
544 (2016). Reelin Regulates the Maturation of Dendritic Spines, Synaptogenesis and Glial
545 Ensheathment of Newborn Granule Cells. *Cereb. Cortex* 26, 4282–4298. doi:
546 10.1093/cercor/bhw216.
- 547 Chen, Y., Beffert, U., Ertunc, M., Tang, T.-S., Kavalali, E. T., Bezprozvanny, I., et al. (2005). Reelin
548 Modulates NMDA Receptor Activity in Cortical Neurons. *J. Neurosci.* 25, 8209–8216. doi:
549 10.1523/JNEUROSCI.1951-05.2005.
- 550 Cooper, J. A. (2008). A mechanism for inside-out lamination in the neocortex. *Trends Neurosci.* 31,
551 113–119. doi: 10.1016/j.tins.2007.12.003.
- 552 Crittenden, J. R., and Graybiel, A. M. (2011). Basal Ganglia disorders associated with imbalances in
553 the striatal striosome and matrix compartments. *Front. Neuroanat.* 5, 59. doi:
554 10.3389/fnana.2011.00059.
- 555 D’Arcangelo, G., G. Miao, G., Chen, S.-C., Scares, H. D., Morgan, J. I., and Curran, T. (1995). A
556 protein related to extracellular matrix proteins deleted in the mouse mutant reeler. *Nature* 374,
557 719–723. doi: 10.1038/374719a0.
- 558 D’Arcangelo, G., Homayouni, R., Keshvara, L., Rice, D. S., Sheldon, M., and Curran, T. (1999).
559 Reelin is a ligand for lipoprotein receptors. *Neuron* 24, 471–9.
- 560 de Guglielmo, G., Iemolo, A., Nur, A., Turner, A., Montilla-Perez, P., Martinez, A., et al. (2022).
561 Reelin deficiency exacerbates cocaine-induced hyperlocomotion by enhancing neuronal activity
562 in the dorsomedial striatum. *Genes. Brain. Behav.* 21, e12828. doi: 10.1111/gbb.12828.
- 563 Di Chiara, G., and Imperato, A. (1988). Drugs abused by humans preferentially increase synaptic
564 dopamine concentrations in the mesolimbic system of freely moving rats. *Proc. Natl. Acad. Sci.*
565 *U. S. A.* 85, 5274–5278. doi: 10.1073/pnas.85.14.5274.
- 566 Fatemi, S. H., Earle, J. A., and McMenomy, T. (2000). Reduction in Reelin immunoreactivity in
567 hippocampus of subjects with schizophrenia, bipolar disorder and major depression. *Mol.*
568 *Psychiatry* 5, 571,654-663. doi: 10.1038/sj.mp.4000783.
- 569 Fatemi, S. H., Kroll, J. L., and Sary, J. M. (2001). Altered levels of Reelin and its isoforms in
570 schizophrenia and mood disorders. *Neuroreport* 12, 3209–15.

- 571 Fatemi, S. H., Reutiman, T. J., and Folsom, T. D. (2009). Chronic psychotropic drug treatment
572 causes differential expression of Reelin signaling system in frontal cortex of rats. *Schizophr.*
573 *Res.* 111, 138–52. doi: 10.1016/j.schres.2009.03.002.
- 574 Fatemi, S. H., Snow, A. V., Sary, J. M., Araghi-Niknam, M., Reutiman, T. J., Lee, S., et al. (2005).
575 Reelin signaling is impaired in autism. *Biol. Psychiatry* 57, 777–787. doi:
576 10.1016/j.biopsych.2004.12.018.
- 577 Folsom, T. D., and Fatemi, S. H. (2013). The involvement of Reelin in neurodevelopmental
578 disorders. *Neuropharmacology* 68, 122–135. doi: 10.1016/j.neuropharm.2012.08.015.
- 579 Gerfen, C. R. (1992). The neostriatal mosaic: multiple levels of compartmental organization. *Trends*
580 *Neurosci.* 15, 133–9.
- 581 Gernert, M., Hamann, M., Bennay, M., Löscher, W., and Richter, A. (2000). Deficit of striatal
582 parvalbumin-reactive GABAergic interneurons and decreased basal ganglia output in a genetic
583 rodent model of idiopathic paroxysmal dystonia. *J. Neurosci.* 20, 7052–8.
- 584 Gong, S., Doughty, M., Harbaugh, C. R., Cummins, A., Hatten, M. E., Heintz, N., et al. (2007).
585 Targeting Cre recombinase to specific neuron populations with bacterial artificial chromosome
586 constructs. *J. Neurosci. Off. J. Soc. Neurosci.* 27, 9817–9823. doi: 10.1523/JNEUROSCI.2707-
587 07.2007.
- 588 González-Billault, C., Del Río, J. A., Ureña, J. M., Jiménez-Mateos, E. M., Barallobre, M. J.,
589 Pascual, M., et al. (2005). A role of MAP1B in Reelin-dependent neuronal migration. *Cereb.*
590 *Cortex* 15, 1134–1145. doi: 10.1093/cercor/bhh213.
- 591 Graybiel, A. M., Moratalla, R., and Robertson, H. A. (1990). Amphetamine and cocaine induce drug-
592 specific activation of the c-fos gene in striosome-matrix compartments and limbic subdivisions
593 of the striatum. *Proc. Natl. Acad. Sci. U. S. A.* 87, 6912–6916. doi: 10.1073/pnas.87.17.6912.
- 594 Graybiel, A. M., and Ragsdale, C. W. (1978). Histochemically distinct compartments in the striatum
595 of human, monkeys, and cat demonstrated by acetylthiocholinesterase staining. *Proc. Natl.*
596 *Acad. Sci. U. S. A.* 75, 5723–6.
- 597 Grayson, D. R., Jia, X., Chen, Y., Sharma, R. P., Mitchell, C. P., Guidotti, A., et al. (2005). Reelin
598 promoter hypermethylation in schizophrenia. *Proc. Natl. Acad. Sci. U. S. A.* 102, 9341 LP –
599 9346. doi: 10.1073/pnas.0503736102.
- 600 Groc, L., Choquet, D., Stephenson, F. A., Verrier, D., Manzoni, O. J., and Chavis, P. (2007). NMDA
601 Receptor Surface Trafficking and Synaptic Subunit Composition Are Developmentally
602 Regulated by the Extracellular Matrix Protein Reelin. *J. Neurosci.* 27, 10165 LP – 10175. doi:
603 10.1523/JNEUROSCI.1772-07.2007.
- 604 Heiman, M., Schaefer, A., Gong, S., Peterson, J. D., Day, M., Ramsey, K. E., et al. (2008). A
605 Translational Profiling Approach for the Molecular Characterization of CNS Cell Types. *Cell*
606 135, 738–748. doi: 10.1016/j.cell.2008.10.028.
- 607 Hellwig, S., Hack, I., Kowalski, J., Brunne, B., Jarowij, J., Unger, A., et al. (2011). Role for Reelin
608 in neurotransmitter release. *J. Neurosci. Off. J. Soc. Neurosci.* 31, 2352–2360. doi:

- 609 10.1523/JNEUROSCI.3984-10.2011.
- 610 Herkenham, M., and Pert, C. B. (1981). Mosaic distribution of opiate receptors, parafascicular
611 projections and acetylcholinesterase in rat striatum. *Nature* 291, 415–8.
- 612 Herz, J., and Chen, Y. (2006). Reelin, lipoprotein receptors and synaptic plasticity. *Nat. Rev.*
613 *Neurosci.* 7, 850–859. doi: 10.1038/nrn2009.
- 614 Hiesberger, T., Trommsdorff, M., Howell, B. W., Goffinet, A., Mumby, M. C., Cooper, J. A., et al.
615 (1999). Direct binding of Reelin to VLDL receptor and ApoE receptor 2 induces tyrosine
616 phosphorylation of disabled-1 and modulates tau phosphorylation. *Neuron* 24, 481–489. doi:
617 10.1016/s0896-6273(00)80861-2.
- 618 Hirota, Y., and Nakajima, K. (2017). Control of Neuronal Migration and Aggregation by Reelin
619 Signaling in the Developing Cerebral Cortex. *Front. cell Dev. Biol.* 5, 40. doi:
620 10.3389/fcell.2017.00040.
- 621 Holt, D. J., Herman, M. M., Hyde, T. M., Kleinman, J. E., Sinton, C. M., German, D. C., et al.
622 (1999). Evidence for a deficit in cholinergic interneurons in the striatum in schizophrenia.
623 *Neuroscience* 94, 21–31.
- 624 Howell, B. W., Hawkes, R., Soriano, P., and Cooper, J. A. (1997). Neuronal position in the
625 developing brain is regulated by mouse disabled-1. *Nature* 389, 733–737. doi: 10.1038/39607.
- 626 Howell, B. W., Herrick, T. M., and Cooper, J. A. (1999). Reelin-induced tyrosine [corrected]
627 phosphorylation of disabled 1 during neuronal positioning. *Genes Dev.* 13, 643–8.
- 628 Impagnatiello, F., Guidotti, A. R., Pesold, C., Dwivedi, Y., Caruncho, H., Pisu, M. G., et al. (1998).
629 A decrease of reelin expression as a putative vulnerability factor in schizophrenia. *Proc. Natl.*
630 *Acad. Sci. U. S. A.* 95, 15718–23.
- 631 Jossin, Y. (2020). Reelin Functions, Mechanisms of Action and Signaling Pathways During Brain
632 Development and Maturation. *Biomolecules* 10. doi: 10.3390/biom10060964.
- 633 Kang, W.-Y., Kim, S.-S., Cho, S.-K., Kim, S., Suh-Kim, H., and Lee, Y.-D. (2010). Migratory defect
634 of mesencephalic dopaminergic neurons in developing reeler mice. *Anat. Cell Biol.* 43, 241–
635 251. doi: 10.5115/acb.2010.43.3.241.
- 636 Kataoka, Y., Kalanithi, P. S. A., Grantz, H., Schwartz, M. L., Saper, C., Leckman, J. F., et al. (2010).
637 Decreased number of parvalbumin and cholinergic interneurons in the striatum of individuals
638 with Tourette syndrome. *J. Comp. Neurol.* 518, 277–91. doi: 10.1002/cne.22206.
- 639 Kempermann, G. (2008). The neurogenic reserve hypothesis: what is adult hippocampal
640 neurogenesis good for? *Trends Neurosci.* 31, 163–169. doi: 10.1016/j.tins.2008.01.002.
- 641 Kim, H. M., Qu, T., Kriho, V., Lacor, P., Smalheiser, N., Pappas, G. D., et al. (2002). Reelin function
642 in neural stem cell biology. *Proc. Natl. Acad. Sci.* 99, 4020–4025. doi:
643 10.1073/pnas.062698299.
- 644 Krueger, D. D., Howell, J. L., Hebert, B. F., Olausson, P., Taylor, J. R., and Nairn, A. C. (2006).

- 645 Assessment of cognitive function in the heterozygous reeler mouse. *Psychopharmacology*
646 (*Berl*). 189, 95–104. doi: 10.1007/s00213-006-0530-0.
- 647 Lammert, D. B., and Howell, B. W. (2016). RELN Mutations in Autism Spectrum Disorder. *Front.*
648 *Cell. Neurosci.* 10, 84. doi: 10.3389/fncel.2016.00084.
- 649 Lee, G. H., Chhangawala, Z., von Daake, S., Savas, J. N., Yates, J. R., Comoletti, D., et al. (2014).
650 Reelin induces Erk1/2 signaling in cortical neurons through a non-canonical pathway. *J. Biol.*
651 *Chem.* 289, 20307–17. doi: 10.1074/jbc.M114.576249.
- 652 Li, M. J., Wang, P., Liu, X., Lim, E. L., Wang, Z., Yeager, M., et al. (2012). GWASdb: a database
653 for human genetic variants identified by genome-wide association studies. *Nucleic Acids Res.*
654 40, D1047-54. doi: 10.1093/nar/gkr1182.
- 655 Marrone, M. C., Marinelli, S., Biamonte, F., Keller, F., Sgobio, C. A., Ammassari-Teule, M., et al.
656 (2006). Altered cortico-striatal synaptic plasticity and related behavioural impairments in reeler
657 mice. *Eur. J. Neurosci.* 24, 2061–2070. doi: 10.1111/j.1460-9568.2006.05083.x.
- 658 Matsuzaki, H., Minabe, Y., Nakamura, K., Suzuki, K., Iwata, Y., Sekine, Y., et al. (2007). Disruption
659 of reelin signaling attenuates methamphetamine-induced hyperlocomotion. *Eur. J. Neurosci.*
660 25, 3376–3384. doi: 10.1111/j.1460-9568.2007.05564.x.
- 661 McCutcheon, R. A., Brown, K., Nour, M. M., Smith, S. M., Veronese, M., Zelaya, F., et al. (2021).
662 Dopaminergic organization of striatum is linked to cortical activity and brain expression of
663 genes associated with psychiatric illness. *Sci. Adv.* 7. doi: 10.1126/sciadv.abg1512.
- 664 Molnár, Z., Clowry, G. J., Šestan, N., Alzu'bi, A., Bakken, T., Hevner, R. F., et al. (2019). New
665 insights into the development of the human cerebral cortex. *J. Anat.* 235, 432–451. doi:
666 10.1111/joa.13055.
- 667 Nishikawa, S., Goto, S., Hamasaki, T., Ogawa, M., and Ushio, Y. (1999). Transient and
668 compartmental expression of the reeler gene product reelin in the developing rat striatum. *Brain*
669 *Res.* 850, 244–8.
- 670 Nishikawa, S., Goto, S., Yamada, K., Hamasaki, T., and Ushio, Y. (2003). Lack of Reelin causes
671 malpositioning of nigral dopaminergic neurons: evidence from comparison of normal and
672 Reln(rl) mutant mice. *J. Comp. Neurol.* 461, 166–73. doi: 10.1002/cne.10610.
- 673 Niu, S., Yabut, O., and D’Arcangelo, G. (2008). The Reelin signaling pathway promotes dendritic
674 spine development in hippocampal neurons. *J. Neurosci.* 28, 10339–10348. doi:
675 10.1523/JNEUROSCI.1917-08.2008.
- 676 Nullmeier, S., Panther, P., Frotscher, M., Zhao, S., and Schwegler, H. (2014). Alterations in the
677 hippocampal and striatal catecholaminergic fiber densities of heterozygous reeler mice.
678 *Neuroscience* 275, 404–419. doi: 10.1016/j.neuroscience.2014.06.027.
- 679 Olson, L., Seiger, A., and Fuxe, K. (1972). Heterogeneity of striatal and limbic dopamine
680 innervation: highly fluorescent islands in developing and adult rats. *Brain Res.* 44, 283–8.
- 681 Ovadia, G., and Shifman, S. (2011). The Genetic Variation of RELN Expression in Schizophrenia

- 682 and Bipolar Disorder. *PLoS One* 6, e19955. doi: 10.1371/journal.pone.0019955.
- 683 Persico, A. M., D'Agruma, L., Maiorano, N., Totaro, A., Militerni, R., Bravaccio, C., et al. (2001).
684 Reelin gene alleles and haplotypes as a factor predisposing to autistic disorder. *Mol. Psychiatry*
685 6, 150–159. doi: 10.1038/sj.mp.4000850.
- 686 Perugini, M., and Vezina, P. (1994). Amphetamine administered to the ventral tegmental area
687 sensitizes rats to the locomotor effects of nucleus accumbens amphetamine. *J. Pharmacol. Exp.*
688 *Ther.* 270.
- 689 Pujadas, L., Gruart, A., Bosch, C., Delgado, L., Teixeira, C. M., Rossi, D., et al. (2010). Reelin
690 regulates postnatal neurogenesis and enhances spine hypertrophy and long-term potentiation. *J.*
691 *Neurosci.* 30, 4636–4649. doi: 10.1523/JNEUROSCI.5284-09.2010.
- 692 Qiu, S., Korwek, K. M., Pratt-Davis, A. R., Peters, M., Bergman, M. Y., and Weeber, E. J. (2006a).
693 Cognitive disruption and altered hippocampus synaptic function in Reelin haploinsufficient
694 mice. *Neurobiol. Learn. Mem.* 85, 228–242. doi: 10.1016/j.nlm.2005.11.001.
- 695 Qiu, S., Zhao, L. F., Korwek, K. M., and Weeber, E. J. (2006b). Differential reelin-induced
696 enhancement of NMDA and AMPA receptor activity in the adult hippocampus. *J. Neurosci.* 26,
697 12943–12955. doi: 10.1523/JNEUROSCI.2561-06.2006.
- 698 Rapanelli, M., Frick, L. R., and Pittenger, C. (2017). The Role of Interneurons in Autism and
699 Tourette Syndrome. *Trends Neurosci.* 530, 481–484. doi: 10.1016/j.tins.2017.05.004.
- 700 Rice, D. S., and Curran, T. (2001). Role of the reelin signaling pathway in central nervous system
701 development. *Annu. Rev. Neurosci.* 24, 1005–1039. doi: 10.1146/annurev.neuro.24.1.1005.
- 702 Ruzicka, W. B., Zhubi, A., Veldic, M., Grayson, D. R., Costa, E., and Guidotti, A. (2007). Selective
703 epigenetic alteration of layer I GABAergic neurons isolated from prefrontal cortex of
704 schizophrenia patients using laser-assisted microdissection. *Mol. Psychiatry* 12, 385–397. doi:
705 10.1038/sj.mp.4001954.
- 706 Schiffmann, S. N., Jacobs, O., and Vanderhaeghen, J. J. (1991). Striatal restricted adenosine A2
707 receptor (RDC8) is expressed by enkephalin but not by substance P neurons: an in situ
708 hybridization histochemistry study. *J. Neurochem.* 57, 1062–7.
- 709 Sharaf, A., Bock, H. H., Spittau, B., Bouché, E., and Kriegstein, K. (2013). ApoER2 and VLDLr are
710 required for mediating reelin signalling pathway for normal migration and positioning of
711 mesencephalic dopaminergic neurons. *PLoS One* 8, e71091. doi: 10.1371/journal.pone.0071091.
- 712 Sharaf, A., Rahhal, B., Spittau, B., and Roussa, E. (2015). Localization of reelin signaling pathway
713 components in murine midbrain and striatum. *Cell Tissue Res.* 359, 393–407. doi:
714 10.1007/s00441-014-2022-6.
- 715 Sigala, S., Zoli, M., Palazzolo, F., Faccoli, S., Zanardi, A., Mercuri, N. B., et al. (2007). Selective
716 disarrangement of the rostral telencephalic cholinergic system in heterozygous reeler mice.
717 *Neuroscience* 144, 834–844. doi: 10.1016/j.neuroscience.2006.10.013.
- 718 Simó, S., Jossin, Y., and Cooper, J. A. (2010). Cullin 5 regulates cortical layering by modulating the

- 719 speed and duration of Dab1-dependent neuronal migration. *J. Neurosci. Off. J. Soc. Neurosci.*
720 30, 5668–5676. doi: 10.1523/JNEUROSCI.0035-10.2010.
- 721 Simó, S., Pujadas, L., Segura, M. F., La Torre, A., Del Río, J. A., Ureña, J. M., et al. (2007). Reelin
722 induces the detachment of postnatal subventricular zone cells and the expression of the Egr-1
723 through Erk1/2 activation. *Cereb. Cortex* 17, 294–303. doi: 10.1093/cercor/bhj147.
- 724 Sinagra, M., Verrier, D., Frankova, D., Korwek, K. M., Blahos, J., Weeber, E. J., et al. (2005).
725 Reelin, very-low-density lipoprotein receptor, and apolipoprotein E receptor 2 control somatic
726 NMDA receptor composition during hippocampal maturation in vitro. *J. Neurosci. Off. J. Soc.*
727 *Neurosci.* 25, 6127–6136. doi: 10.1523/JNEUROSCI.1757-05.2005.
- 728 Smith, Y., Bevan, M. D., Shink, E., and Bolam, J. P. (1998). Microcircuitry of the direct and indirect
729 pathways of the basal ganglia. *Neuroscience* 86, 353–87.
- 730 Soriano, E., and Del Río, J. A. (2005). The cells of cajal-retzius: still a mystery one century after.
731 *Neuron* 46, 389–394. doi: 10.1016/j.neuron.2005.04.019.
- 732 Strasser, V., Fasching, D., Hauser, C., Mayer, H., Bock, H. H., Hiesberger, T., et al. (2004). Receptor
733 clustering is involved in Reelin signaling. *Mol. Cell. Biol.* 24, 1378–86.
- 734 Stritt, C., and Knöll, B. (2010). Serum response factor regulates hippocampal lamination and dendrite
735 development and is connected with reelin signaling. *Mol. Cell. Biol.* 30, 1828–1837. doi:
736 10.1128/MCB.01434-09.
- 737 Teixeira, C. M., Kron, M. M., Masachs, N., Zhang, H., Lagace, D. C., Martinez, A., et al. (2012).
738 Cell-autonomous inactivation of the reelin pathway impairs adult neurogenesis in the
739 hippocampus. *J. Neurosci.* 32, 12051–12065. doi: 10.1523/JNEUROSCI.1857-12.2012.
- 740 Teixeira, C. M., Martín, E. D., Sahún, I., Masachs, N., Pujadas, L., Corvelo, A., et al. (2011).
741 Overexpression of Reelin prevents the manifestation of behavioral phenotypes related to
742 schizophrenia and bipolar disorder. *Neuropsychopharmacology* 36, 2395–2405. doi:
743 10.1038/npp.2011.153.
- 744 Todtenkopf, M. ., Stellar, J. ., Williams, E. ., and Zahm, D. . (2004). Differential distribution of
745 parvalbumin immunoreactive neurons in the striatum of cocaine sensitized rats. *Neuroscience*
746 127, 35–42. doi: 10.1016/j.neuroscience.2004.04.054.
- 747 Torrey, E. F., Barci, B. M., Webster, M. J., Bartko, J. J., Meador-Woodruff, J. H., and Knable, M. B.
748 (2005). Neurochemical markers for schizophrenia, bipolar disorder, and major depression in
749 postmortem brains. *Biol. Psychiatry* 57, 252–260. doi: 10.1016/j.biopsych.2004.10.019.
- 750 Tueting, P., Costa, E., Dwivedi, Y., Guidotti, A., Impagnatiello, F., Manev, R., et al. (1999). The
751 phenotypic characteristics of heterozygous reeler mouse. *Neuroreport* 10, 1329–34.
- 752 Varela, M. J., Lage, S., Caruncho, H. J., Cadavid, M. I., Loza, M. I., and Brea, J. (2015). Reelin
753 influences the expression and function of dopamine D2 and serotonin 5-HT2A receptors: a
754 comparative study. *Neuroscience* 290, 165–174. doi: 10.1016/j.neuroscience.2015.01.031.
- 755 Vaswani, A. R., Weykopf, B., Hagemann, C., Fried, H.-U., Brüstle, O., and Blaess, S. (2019).

756 Correct setup of the substantia nigra requires Reelin-mediated fast, laterally-directed migration
757 of dopaminergic neurons. *Elife* 8. doi: 10.7554/eLife.41623.

758 Vílchez-Acosta, A., Manso, Y., Cárdenas, A., Elias-Tersa, A., Martínez-Losa, M., Pascual, M., et al.
759 (2022). Specific contribution of Reelin expressed by Cajal-Retzius cells or GABAergic
760 interneurons to cortical lamination. *Proc. Natl. Acad. Sci. U. S. A.* 119, e2120079119. doi:
761 10.1073/pnas.2120079119.

762 Wang, Z., Hong, Y., Zou, L., Zhong, R., Zhu, B., Shen, N., et al. (2014). Reelin gene variants and
763 risk of autism spectrum disorders: An integrated meta-analysis. *Am. J. Med. Genet. Part B*
764 *Neuropsychiatr. Genet.* 165, 192–200. doi: 10.1002/ajmg.b.32222.

765 Yasui, N., Nogi, T., and Takagi, J. (2010). Structural Basis for Specific Recognition of Reelin by Its
766 Receptors. *Structure* 18, 320–331. doi: 10.1016/j.str.2010.01.010.

767 Zhao, C., Deng, W., and Gage, F. H. (2008). Mechanisms and Functional Implications of Adult
768 Neurogenesis. *Cell* 132, 645–660. doi: 10.1016/j.cell.2008.01.033.

769

770 **Data Availability Statement**

771 The original contributions presented in the study are included in the article/supplementary material,
772 further inquiries can be directed to the corresponding author/s.

773 **Figure Legends**

774 **Figure 1. Reelin in the striatum is mainly expressed by D1 striatonigral MSNs.**

775 Immunohistochemistry against Reelin shows that Reelin protein is absent in the striatum of Cre fR/fR
776 mice (B) compared to the controls (A) while it is clearly overexpressed in the striatum of TgRln mice
777 (D) compared to controls (C). Quantification of Reelin mRNA levels in the Dorsal striatum (E) and
778 NAcc (F) of D1/D2-TRAP mice (n=3-4). Quantification of Dab1 mRNA levels in the Dorsal
779 striatum (G) and NAcc (H) of D1/D2-TRAP mice (n=4-7). NAcc, Nucleus Accumbens; D1,
780 Dopamine 1 Receptor; D2, Dopamine 2 Receptor. Statistical analysis was performed using Student's
781 t-test; significant differences were established at *p<0.05, **p<0.01. Data represents mean±SEM.

782 **Figure 2. Striatal MSNs density and organization is not affected by Reelin levels.**

783 Representative images of Darpp-32 immunohistochemistry (striatal MSNs) in coronal sections of
784 control and Cre fR/fR (A-B) and control and TgRln (C-D) striatum. Quantification of Darpp-32 cell
785 density showed no alterations of striatal MSNs neither in Cre fR/fR (n=5-6) (E) nor in TgRln (n=6)
786 (F) mice. Immunofluorescence for μ -Opioid receptor (MOR) in coronal sections of control (G), Cre
787 fR/fR (H) and TgRln (I) striatum showing a similar organization of striatal patches in all the models.
788 Statistical analysis was performed using Student's t-test. Data is represented as mean±SEM.

789 **Figure 3. Reelin overexpression increased the density of striatal cholinergic interneurons.**

790 Immunohistochemistry of ChAT in striatal coronal sections of control and Cre fR/fR mice (A-B),
791 with representative subdivision of the striatum in four regions (DM, Dorsal-Medial; DL, Dorsal-
792 Lateral; VM, Ventral-Medial; VL, Ventral-Lateral). Quantification of ChAT density in the striatal
793 subdivisions showed no differences between control and Cre fR/fR mice (n=4) (C-F). Representative
794 images of ChAT immunohistochemistry in the striatum of control and TgRln mice, with higher
795 magnification insets showing increased ChAT+ neuronal density in the TgRln mice (G-H).

796 Quantification of ChAT cell density indicated a significant increase in the DL, VL and DM striatal
797 regions of TgRln mice (n=4-6) (**I-L**). Statistical analyses were performed using Student's t-test;
798 *p<0.05. Data is represented as mean±SEM.

799 **Figure 4. Increased levels of Reelin alter the density of Parvalbumin interneurons in the**
800 **ventral-medial striatum.**

801 Immunohistochemistry for PV in coronal sections of control and Cre fR/fR striatum (**A-B**),
802 subdividing the striatum in four regions (DM, Dorsal-Medial; DL, Dorsal-Lateral; VM, Ventral-
803 Medial; VL, Ventral-Lateral). Quantification of the density of PV interneurons indicated no
804 differences between the control and Cre fR/fR mice (n=4) (**C-F**). Representative images of PV
805 immunostaining in the striatum of control and TgRln mice (**G-H**). Quantification of PV
806 immunohistochemistry indicated an increase in the density of PV positive cells in the VL striatum of
807 TgRln mice (n=4-5) (**K**) with no differences in the other striatal regions (**I-J, L**). Statistical analyses
808 were performed using Student's t-test; *p<0.05. Data is represented as mean±SEM.

809
810 **Figure 5. Increase of Reelin expression elevates dopaminergic projections in the Ventral**
811 **Striatum.**

812 Immunohistochemistry for TH to stain dopaminergic projections in coronal sections of the DS, NAcc
813 and OT of control and Cre fR/fR mice (**A-B**). TH intensity remains constant in the striatum (**C**),
814 NAcc (**D**) and OT (**E**) of Cre fR/fR mice compared to controls (n=4) (**C-E**). Immunohistochemistry
815 for TH in control and TgRln mice (**F-G**). Increased TH immunoreactivity was detected in the NAcc
816 (**I**) and OT (**J**) but not in the DS (**H**) of TgRln mice compared to controls (n=8-14). NAcc, Nucleus
817 Accumbens; OT, Olfactory Tubercle. Statistical analyses were performed using Student's t-test;
818 **p<0.01; ***p<0.001. Results represent the mean±SEM.

819 **Figure 6. Increased number of dopaminergic synaptic boutons in the NAcc of TgRln mice.**

820 Immunohistochemistry for TH staining dopaminergic synaptic boutons in the dorsal (**A, E**) and
821 ventral regions (**B, F**) of the DS, NAcc (**C, G**) and OT (**D, H**) of TgRln mice and its controls.
822 Quantification of the density of dopaminergic boutons evidenced a higher density of synaptic
823 boutons in the NAcc (**K**) of TgRln mice compared to its controls while no differences were observed
824 in the rest of the analysed structures (**I-J, L**). DS, Dorsal striatum; NAcc, Nucleus Accumbens; OT,
825 Olfactory Tubercle. Statistical analyses were performed using Student's t-test; *p<0.05. Data is
826 represented as mean±SEM.

827 **Figure 7. Schematic summary of the striatal organization in different Reelin mouse models.**

828 Density of striatal MSNs is preserved between the control, Cre fR/fR and TgRln striatums. Although
829 the density of striatal PV-positive and ChAT-positive interneurons is maintained between control and
830 Cre fR/fR mice, it is increased in the DS of TgRln mice. Increased numbers of ChAT-positive
831 interneurons are present in the Dorsal striatum and higher numbers of PV-positive interneurons are
832 distributed in the Ventral Medial striatum sub-region. Dopaminergic projections are represented with
833 different gradient of brown colour, showing a specific increase of TH fibrils in the NAcc and OT of
834 the TgRln mice compared with controls.

835

FIGURE 1

bioRxiv preprint doi: <https://doi.org/10.1101/2023.01.21.525025>; this version posted January 22, 2023. The copyright holder for this preprint (which was not certified by peer review) is the author/funder. All rights reserved. No reuse allowed without permission.

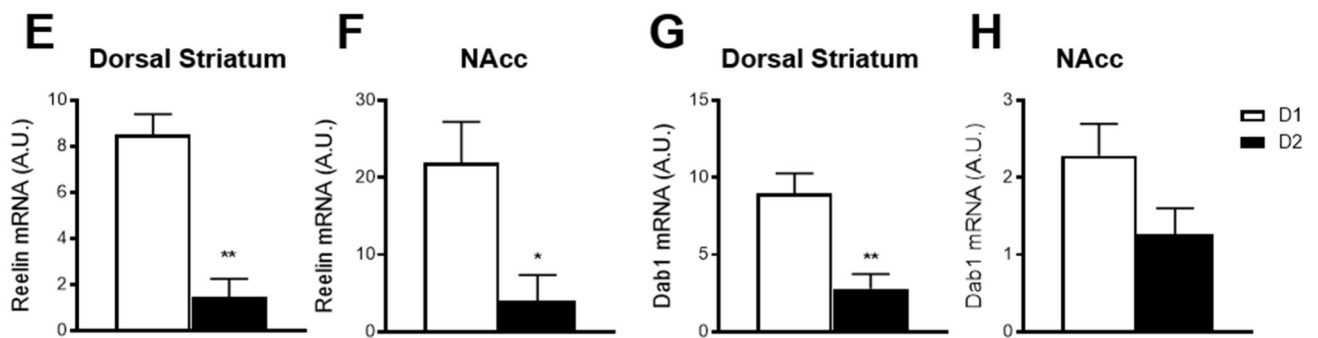
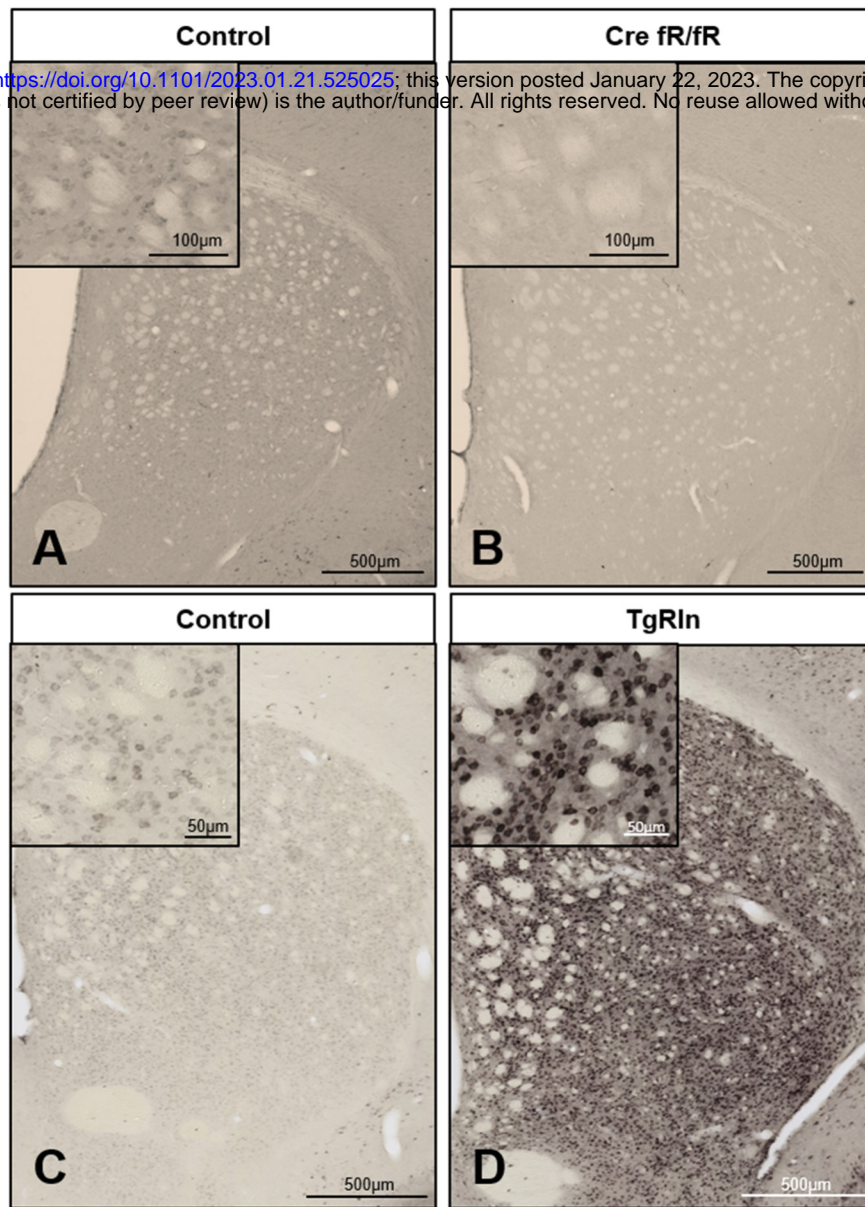


FIGURE 2

bioRxiv preprint doi: <https://doi.org/10.1101/2023.01.21.525025>; this version posted January 22, 2023. The copyright holder for this preprint (which was not certified by peer review) is the author/funder. All rights reserved. No reuse allowed without permission.

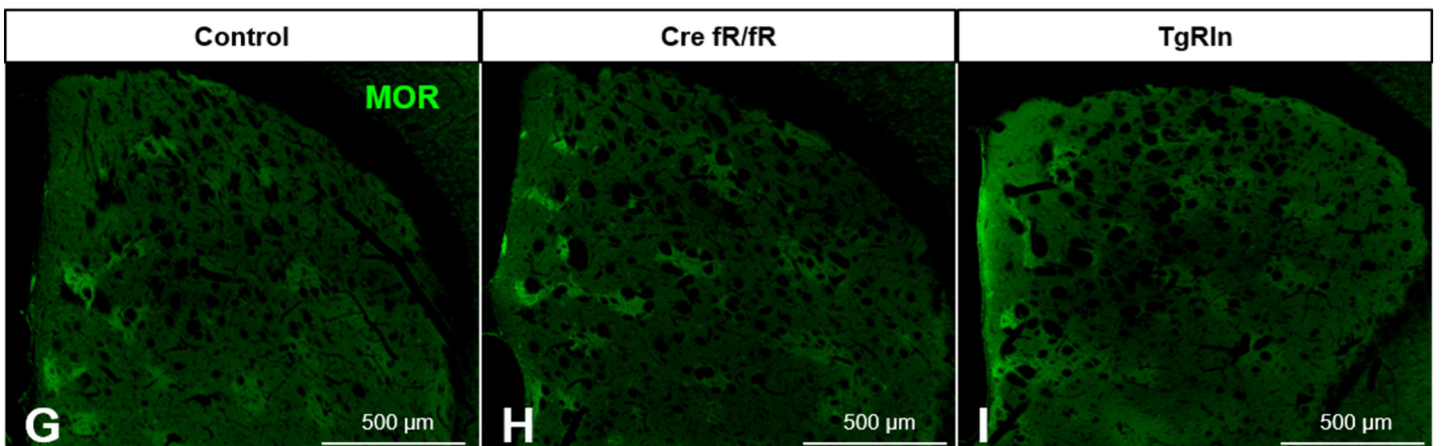
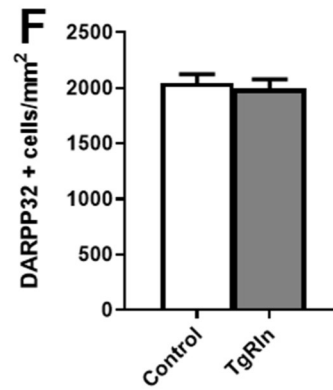
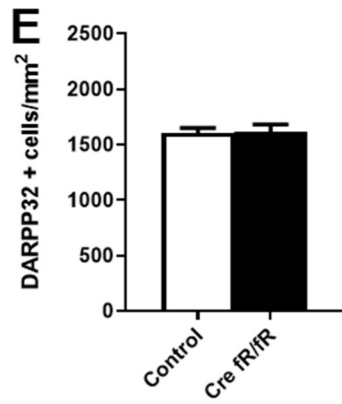
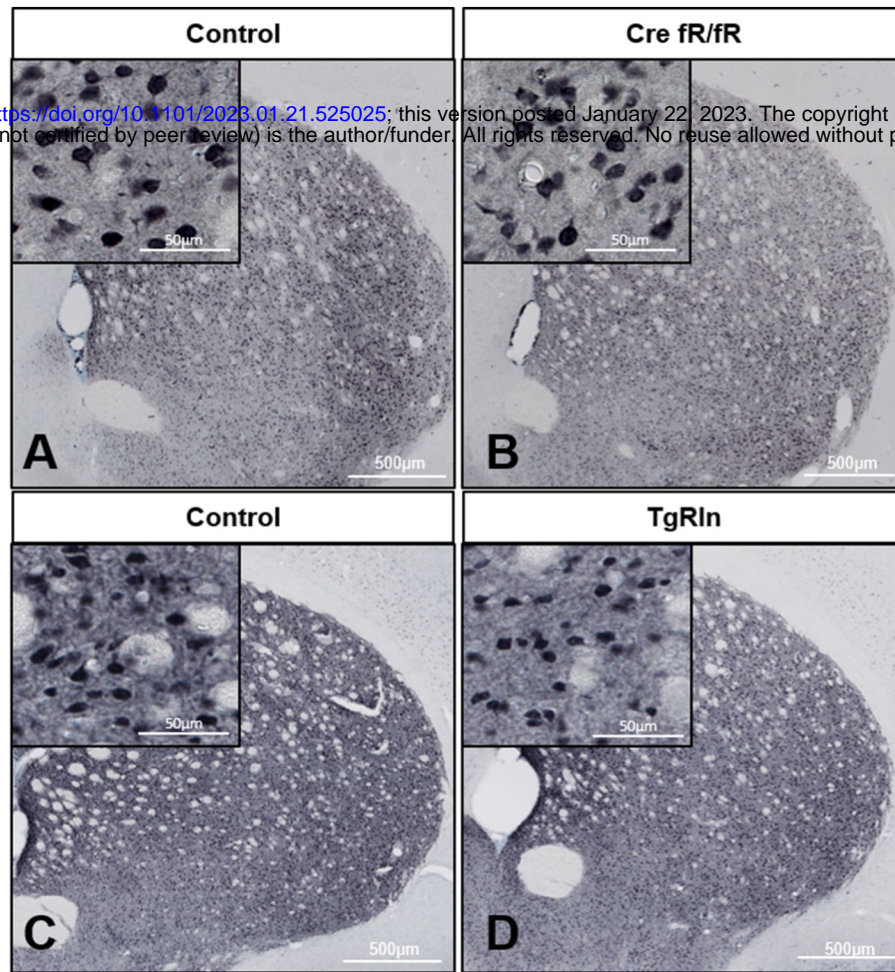


FIGURE 3

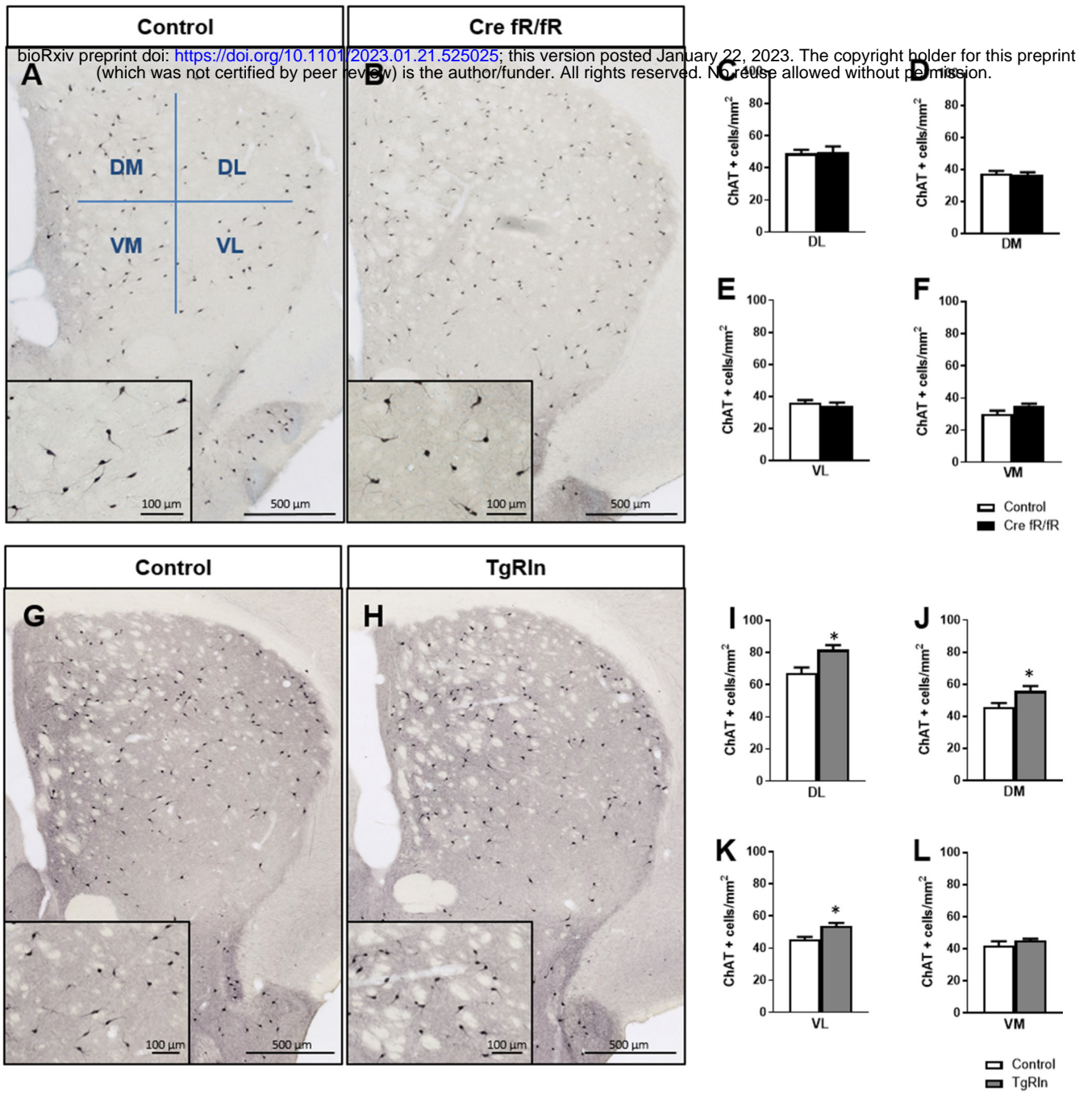


FIGURE 4

bioRxiv preprint doi: <https://doi.org/10.1101/2023.01.21.525025>; this version posted January 22, 2023. The copyright holder for this preprint (which was not certified by peer review) is the author/funder. All rights reserved. No reuse allowed without permission.

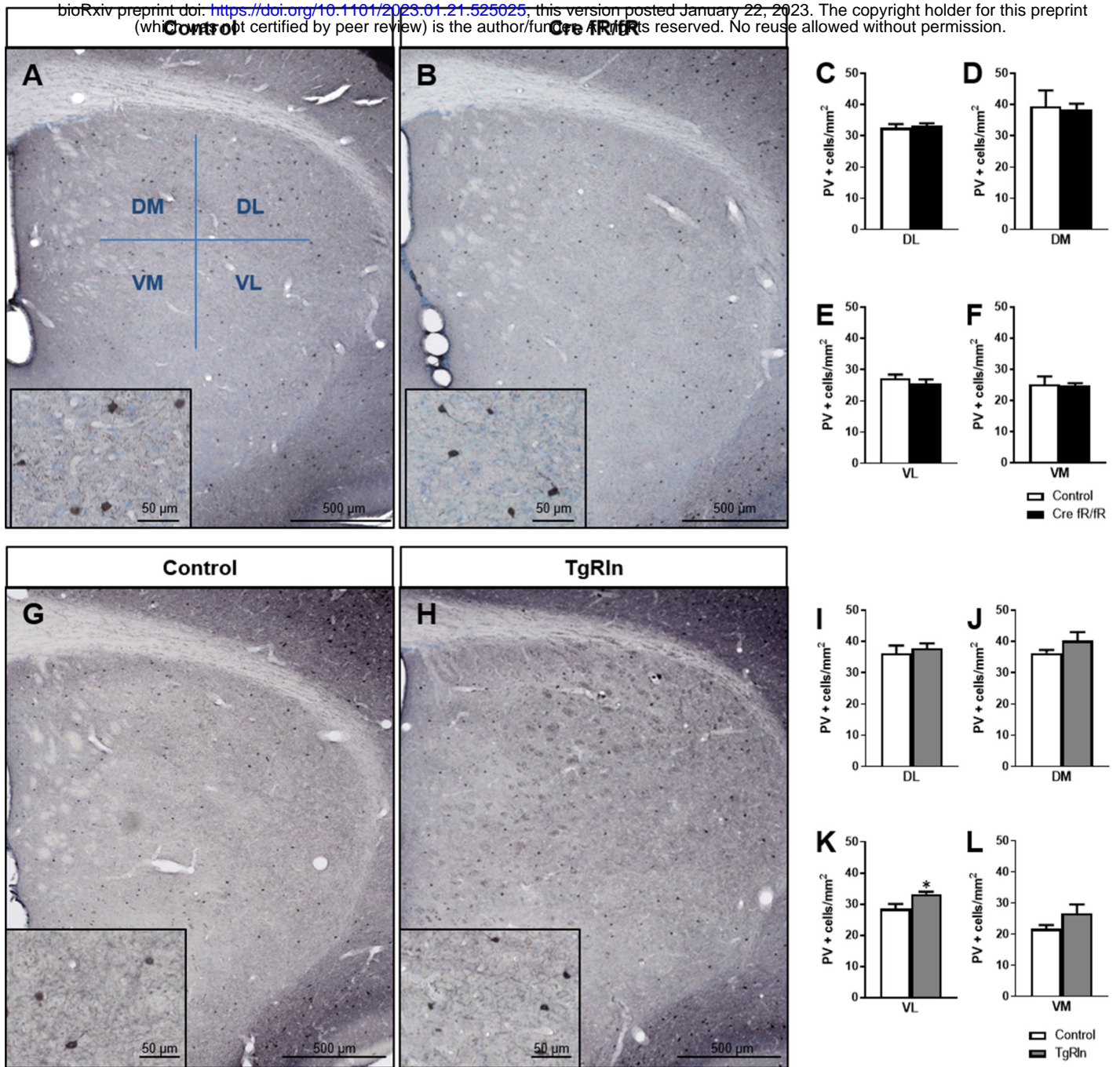


FIGURE 5

bioRxiv preprint doi: <https://doi.org/10.1101/2023.01.21.525025>; this version posted January 22, 2023. The copyright holder for this preprint (which was not certified by peer review) is the author/funder. All rights reserved. No reuse allowed without permission.

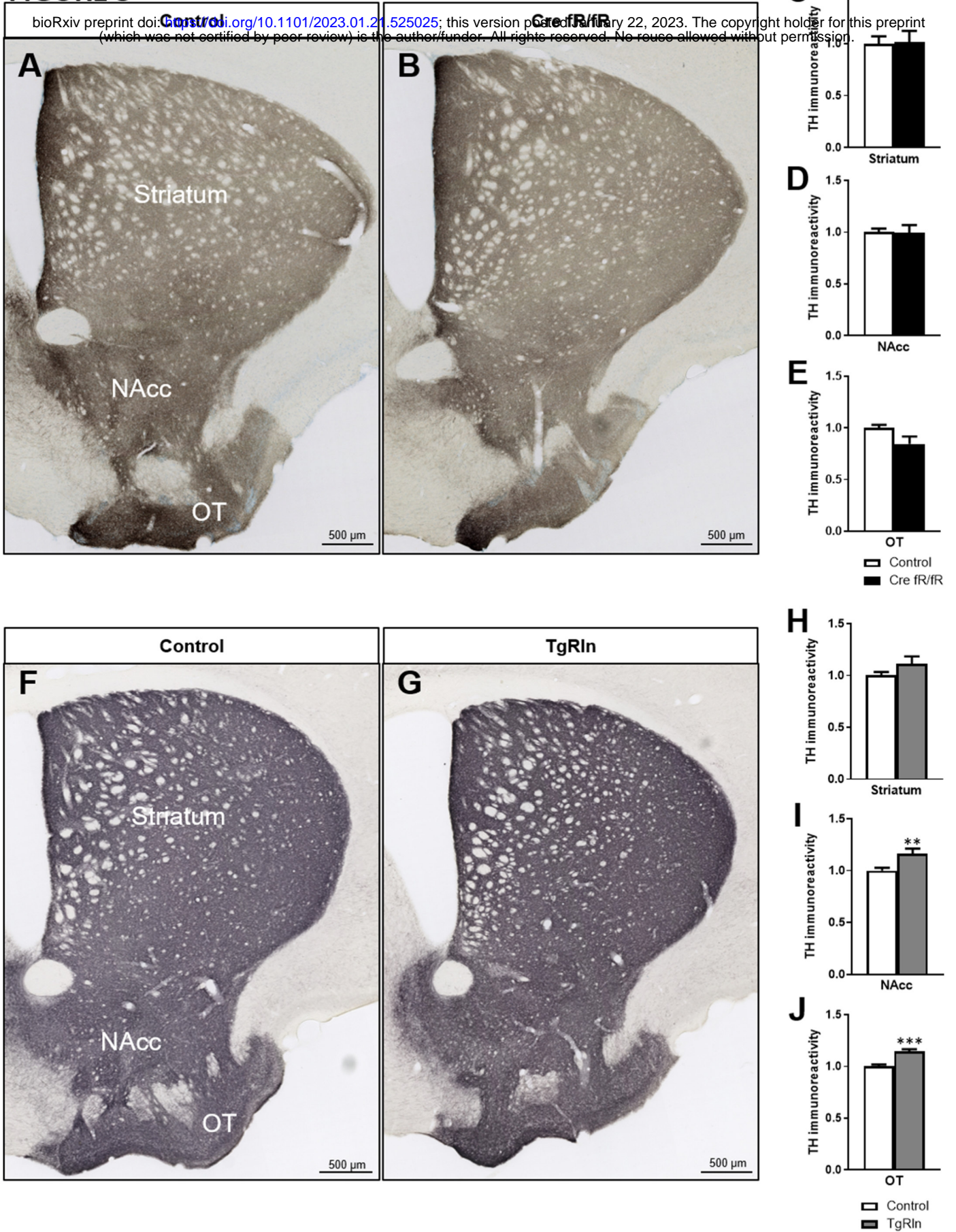


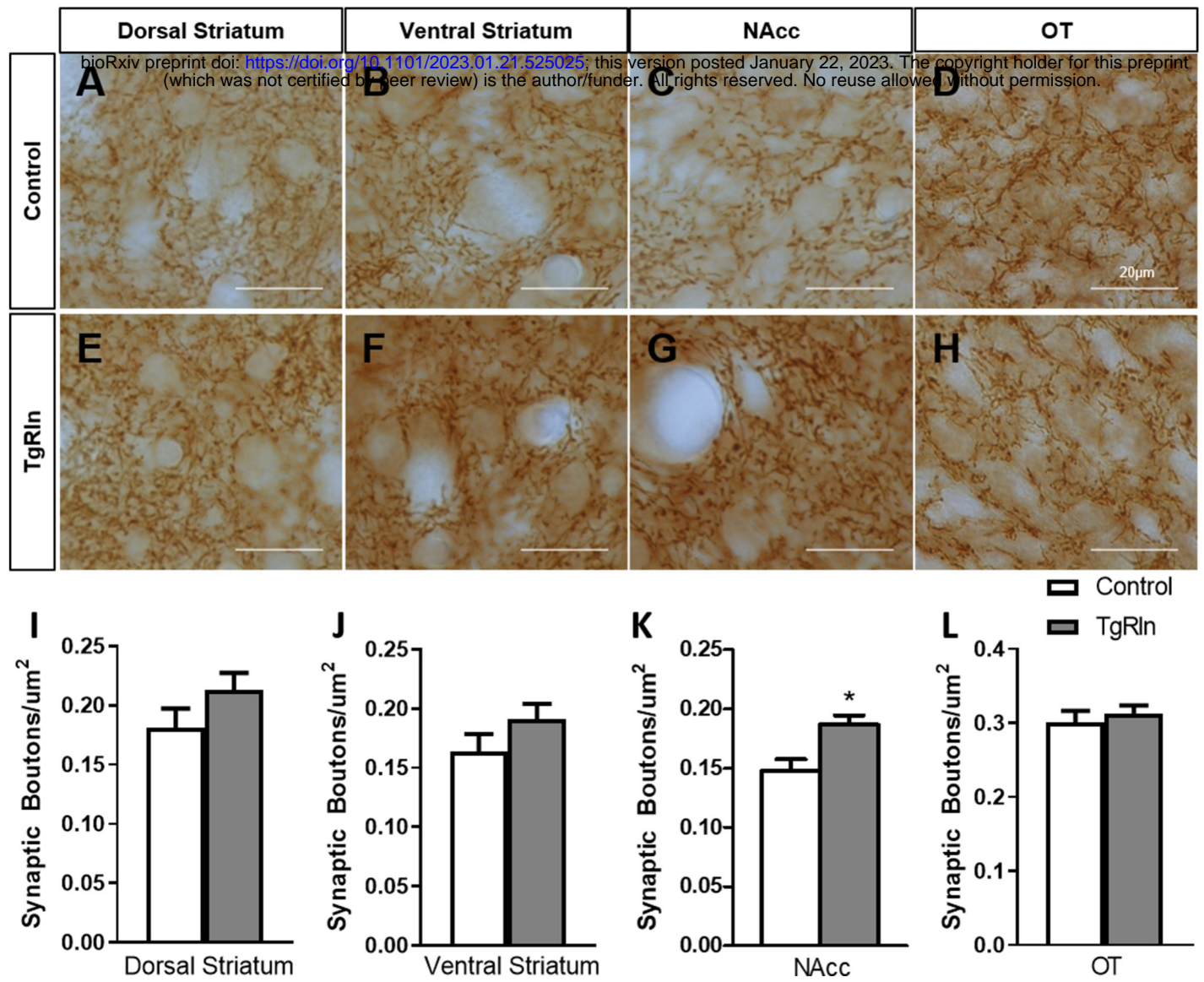
FIGURE 6

FIGURE 7

